REDUCED ENERGY CONSUMPTION EVAPORATOR FOR USE IN DESALTING IMPAIRED WATERS

by

B. W. Tleimat and M. C. Tleimat

WATERREUSETECHNOLOGY
75 Ina court
Alamo, California 94507

Contract No. 1425-3-CR-19560
Technical Completion Report
June 1995

Water Treatment Technology Report No. 11

U.S. Department of the Interior
Bureau of Reclamation
Denver Office
Technical Service Center
Environmental Resources Team
Water Treatment Engineering and Research Group

REPORT DOCUMENTATION PAGE

Form Approved OMB NO 0704-0188

1. AGENCY USE ONLY *(Leave Blank)*	2. REPORT DATE	3. REPORT TYPE AND DATES COVERED
	June 1995	Final

4. TITLE AND SUBTITLE
Reduced Energy Consumption Evaporator for Use in Desalting Impaired Waters

6. FUNDING NUMBERS
Contract No. 1425-3-CR-19560

6. AUTHOR(S)
B.W. Tleimat and M.C. Tleimat

7. PERFORMING ORGANIZATION NAME(S) AND ADDRESS(ES)
Water Reuse Technology (WRT)
75 Ina Court
Alamo, California 94507

8. PERFORMING ORGANIZATION REPORT NUMBER

9. SPONSORING/MONITORING AGENCY NAME(S) AND ADDRESS(ES)
Co-sponsored by WRT and the Bureau of Reclamation,
Denver Federal Center
PO Box 25007
Denver, CO 802250007

10. SPONSORING/MONITORING AGENCY REPORT NUMBER
Water Treatment Technology Program Report No. 11

II. SUPPLEMENTARY NOTES

12a. DISTRIBUTI ON/AVAILABILITY STATEMENT
Available from the National Technical Information Service, Operations Division, 5285 Port Royal Road Springfield, Virginia 22161

12b. DISTRIBUTION CODE

13. ABSTRACT *(Maximum 200 words)*

The basic objective of tbis program is to demonstrate significant savings in energy consumption by the use of the wiped filn rotating disk (WFRD) evaporator in a five-effect vapor compression distillation (MEVCD) system to recover the maximun amount of water from agricultural drainage water and other impaired waters. Tests were conducted using a 10,000 ppn aqueous solution of sodium sulfate and sodium chloride to simulate the composition of agricultural drainage water in the San Joaquin Valley, Califomia. The feed was concentrated by a factor ranging from 15 to 20 resulting in a blowdown salinity o 150,000 to 200,000 ppm. The results showed the presence of dissolved salts has significant influence on energy consumption by the compressor of e commercial 60,000 gal/day VCD unit tested at Los Banos, California. The specific energy consumption by the rotor was found to be a function of condensate flux. At a design flux of 38 kg/hrm^2, the energy consumption by the rotor i expected to be as low as 3.2 kWhr/m^3 (42 kWhr/kgal) for rotor and compressor.

14. SUBJECT TERMS-
desalting/distillation/
agricultural drainage/ii waters/San Joaquin Valley

16. NUMBER OF PAGES
41

16. PRICE CODE

17. SECURITY CLASSIFICATION OF REPORT	18. SECURITY CLASSIFICATION OF THIS PAGE	19. SECURITY CLASSIFICATION OF ABSTRACT	20. LIMITATION OF ABSTRACT
UL	UL	UL	UL

REDUCED ENERGY CONSUMPTION EVAPORATOR FOR USE IN DESALTING IMPAIRED WATERS

by

'B. W. Tleimat and M. C. Tleimat

WATERREUSETECHNOLOGY
75 Ina court
Alamo, California 94507

Contract No. 1425-3-CR-19560
Technical Completion Report
June 1995

Water Treatment Technology Report No. 11

U.S. Department of the Interior
Bureau of Reclamation
Denver Office
Technical Service Center
Environmental Resources Team
Water Treatment Engineering and Research Group

Bureau of Reclamation
Mission Statement

The mission of the Bureau of Reclamation is to manage, develop, and protect water and related resources in an environmentally and economically sound manner in the interest of the American public.

U.S. Department of the Interior
Mission Statement

As the Nation's principal conservation agency, the Department of the Interior has responsibility for most of our nationally-owned public lands and natural resources. This includes fostering sound use of our land and water resources; protecting our fish, wildlife, and biological diversity; preserving the environmental and cultural values of our national parks and historical places; and providing for the enjoyment of life through outdoor recreation. The Department assesses our energy and mineral resources and works to ensure that their development is in the best interests of all people by encouraging stewardship and citizen participation in their care. The Department also has a major responsibility for American Indian reservation communities and for people who live in island territories under U.S. Administration.

Disclaimer

The informatioa contained in this report regarding commercial products or firms may not be used for advertising or promotional purposes and is not to be construed as au endorsement of any product or firm by the Bureau of Reclamation.

The information contained in this report was developed for the Bureau of Reclamation: a0 warranty as to the accuracy, usefulness, or completeness is expressed or implied.

TABLE OF CONTENTS

LIST OF FIGURES & TABLES

Abstract

The basic objective of this program is to demonstrate significant savings in energy consumption in the use of the wiped film rotating disk (WFRD) evaporator in multi-effect vapor compression distillation (MEVCD) system in the recovery of the maximum amount of water from agricultural drainage water and other impaired waters. The use of WFRD evaporator results in very high overall heat transfer coefficient, U, that allows the use of small overall temperature difference across the heat transfer surface and the use of MEVCD allows gradual increase of brine salinity in each effect thus reducing the effects of brine concentration in comparison to single effect vapor compression distillation (SEVCD) systems. These two factors in combination result in significant reduction in heat transfer area in the evaporator as well as reduction% energy consumption in comparison to conventional shell and tube SEVCD systems.

Two sets of tests were conducted. One set was conducted using distilled water feed and the second set was conducted using a 10,000 ppm aqueous solution of sodium sulfate and sodium chloride. The objective was to simulate the composition of agricultural drainage water in the San Joaquin Valley in California with calcium and magnesium deleted to avoid scale on the heat transfer surfaces. The results from the first set were used as a baseline for comparison with the results from the second set. In the second set, the feed was concentrated by a factor ranging from 15 to 20 resulting in a blowdown salinity of 150,000 to 200,000 ppm.

The results from these two sets showed that the presence of dissolved salts influenced the value of U in the five effect evaporator due to lower thermal conductivity and higher viscosity of the brine. The value of U ranged from about 12 to 18 kW/° Cm' (2000 to 3000 Btu/hr° Fft') in the temperature range of 32 - 55° C (90 to 130" F). The results from the second set showed that the presence of dissolved salts has significant influence on specific energy consumption by the compressor per unit of distillate from the plant. The specific energy consumption averaged about 6 kWhr/m^3 of distilled water product (21 kWhr/kgal) for the first set and averaged about 8 kWhr/m^3 (29 kWhr/kgal) for the second set. This figure is about 30 percent of the specific energy consumed by the compressor of a commercial 50,000 gal/day SEVCD unit tested by Bechtel National, Inc. (1) for the State of California Department of Water Resources at Los Banos, California.

The specific energy consumption by the rotor was found to be a function of condensate flux. Low flux resulted in high specific energy consumption and high flux resulted in low specific energy consumption. At the design flux of 38 kg/hrm^2 (7.5 lbs/hrft^2), the energy consumption by the rotor is expected to be as low as 3.2 kWhr/m^3 (12 kWhr/kgal) for both types of feeds..

Nomenclature

A	Area of heat transfer surface	m^2
C_p	Specific heat of vapor at constant pressure	kJ/kg°C
Dt	Temperature difference	°C
E_{is}	Calculated isentropic specific energy consumption by compressor	kWh/kgal
E_c	Measured energy consumption by rotor	kWh/kgal
E_t	Measured energy consumption by rotor and compressor	kWh/kgal
F	Measured condensate flux	lbs/hft²
m_b	Brine blowdown mass rate	kg/hr
m_d	Distillate mass rate	kg/hr
P	Absolute pressure in evaporator	bars
R	Gas constant for water vapor	kJ/kg°C
S_b	Brine salinity	ppm
S_f	Feed salinity	ppm
t	Temperature	°C
T	Absolute temperature	°K
U	Overall heat transfer coefficient	kW/m²°C
W	Isentropic compressor work in SEVCD	kJ/kg
W_5	Isentropic compressor work in S-effect VCD	kJ/kg
W_n	Isentropic compressor work in n-effect VCD	kJ/kg
α	Boiling point elevation	°C
r	Latent heat of condensation	kJ/kg

Introduction

The management of agricultural drainage water is a pressing problem for many parts of the globe. The problem of disposing of this water in California is of great concern to California agriculture. It is estimated (2) that by the beginning of the next century, the annual drainage in California may reach 453 million m^3 (120 billion U.S. gallons). The California Department of Water Resources is conducting a research and development program to recover about 95 percent of this water for reuse by desalination and the brine would be collected in salt gradient solar ponds. These ponds collect solar energy which can be extracted in the form of thermal energy that can be used to drive a distillation system or converted to electromechanical energy to drive other desalination systems. The total aggregate capacity of such plants would be in excess of 1.3 million m^3/day (340 million U. S. gal/day). At an estimated energy requirement of 10 kWhr/m^3 (37.85 kWh/kgal) of desalted water, the capacity of the power plants to supply this energy would be in excess of 2000 megawatts. Any process or combination of processes that can reduce the energy required to desalt this water would result in great savings in capital cost of the power plant as well as operating expenses of the desalting plant. It is believed that a hybrid reverse osmosis (RO) and distillation process is being considered by the State. RO would recover 50 to 80 percent of this water and distillation would recover the balance from the RO brine.

SEVCD is gaining acceptance in applications requiring zero discharge from desalination and power plants at inland locations. In power plants, the blowdown from cooling towers or other impaired water is fed either to a combination of RO and VCD or VCD alone to recover most of the water for reuse and the balance is fed to crystallizers to evaporate the balance of the water. At inland desalination plants the reject brine from an RO plant would be fed to a VCD plant to reduce its volume and the concentrated blowdown is fed into evaporation ponds or crystallizers. In a recent application (3) in Australia, owners of two power plants used RO and VCD in the first plant to treat the blowdown from cooling waters for zero discharge, however, after reviewing the data from the first plant, the owners decided to use VCD only in the second plant instead of combined RO and VCD. It is believed that their decision was based on economic comparison and simplicity.

Thermodynamic analysis (4) shows that the use of MEVCD will result in energy saving in comparison to SEVCD in the desalting of saline waters; the higher the recovery the larger the energy saving. The saving results from the gradual increase of salinity in each effect of the MEVCD in comparison to SEVCD. This program was designed to show these effects and produce data on heat transfer coefficient and energy requirement on the use of WFRD evaporator in the temperature range of 30 to 60° C (86 - 140° F). This range was selected to assess the potential use of extracted thermal energy from salt gradient solar ponds to drive multieffect distillation (MED) plants.

Vapor Compression Distillation

Figure 1 shows the flow diagram for a single effect VCD process and Fig. 2 shows the corresponding temperature entropy diagram for the process shown on Fig; 1. In an ideal system, preheated feed water enters the evaporator where part of it evaporates at state point 1 and the balance is withdrawn as blowdown at state point 4. The generated vapor at state point 1 is compressed by the compressor to raise its saturation pressure and temperature to state point 2 and then is condensed on the heat transfer surface HTS to release its latent heat of condensation with the condensate taken out at state point 3. The released latent heat of condensation is transferred across heat transfer surface I-ITS to supply the latent heat of evaporation to the feed stream so that no external source of vapor is required. Thus, the major energy required to drive this process is that required by the compressor to compress. the vapor from state point 1 to state point 2.

Assuming that the water vapor behaves as an ideal gas and neglecting friction losses in the piping, the isentropic compression work required by the compressor is given by:

$$W = C_p T [(P_2/P_1)^{R/Cp} - 1] \quad (1)$$

Here, the pressure rise from P_1 to P_a overcomes the effects of dissolved solids

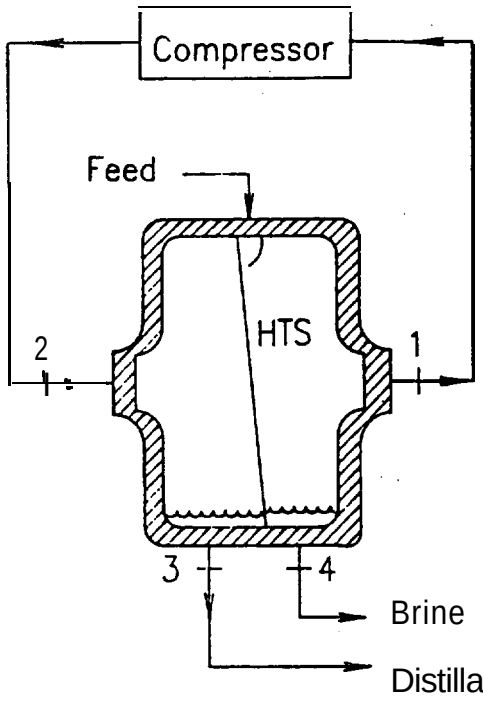

Figure 1. Schematic diagram of basic vapor compression system.

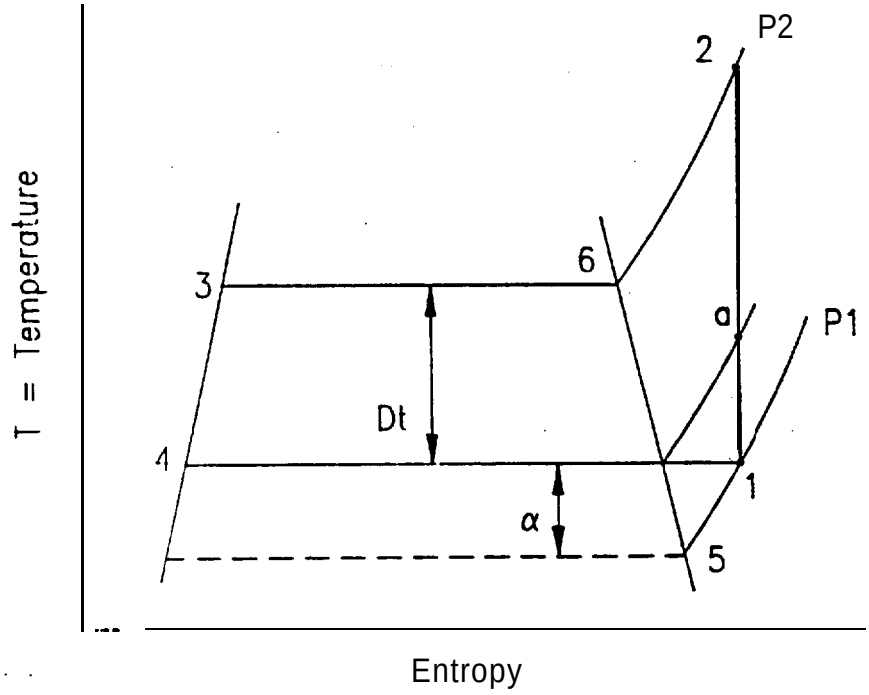

Figure 2. Tempera ture - entropy diagram corresponding to the process shown in figure 1.

in the solution in the evaporator and the pressure rise from P_a to P_2 supplies the temperature difference Dt to drive the latent heat of condensation across the heat transfer surface.

The Clausius Clapeyron equation (5) relates the saturation pressure and saturation temperature along the saturation vapor line by the equation:

$$dP/P = (r/R)(dT/T^2) \quad (2)$$

Integrating this equation from P_1 to P_2 results in:

$$\ln P_2/P_1 = (r/R)(T_6 - T_5)/T_5T_6 \quad (3)$$

however $T_6 - T_5$ = Dt + a ; T_6 = T + Dt and T_5 = T - α where a is the boiling point elevation due to the presence of dissolved solids in the solution. Because Dt and a are small compared to T one can write $T_5T_6 \approx T^2$ and combining Equations 1 and 3 results in:

$$W = C_pT\ [\text{Exp}\ \{r(Dt + \alpha)/C_pT^2\} - 1] \quad (4)$$

Recalling that Exp X can be expanded into infinite series as:

Exp x = 1 + x + $X^2/2!$ + $X^3/3!$ + ...

for small values of $r(Dt + \alpha)/C_pT^2 \leq 0.05$ one can neglect all high order terms and Eq. 4 reduces to the simple relation:

$$W = r(Dt + \alpha)/T \quad (5)$$

for values higher than 0.05 it is recommended that Eq. 1 or Eq. 4 be used for more accurate estimates.

Multieffect Vapor Compression Distillation

Figure 3 shows the flow diagram for a five effect VCD system and Fig. 4 shows the temperature entropy diagram corresponding to the process shown on Fig. 3. In this system heat transfer surfaces A, B, C, D, and E represent the heat transfer surfaces in each of the five effects. The feed enters the first effect at point a and is spread on heat transfer A where part of it evaporates and the balance is taken out by pump P1 and introduced into the second effect at point b. This process is repeated in effects 2, 3, 4, and 5, however, the effluent from P5 is discharged as concentrated blowdown. The vapor generated in effect 1 is used as the heating vapor in effect 2 and the vapor generated in effect 2 is used as the heating vapor in effect 3 and so on until the fifth effect where the vapor generated in the fifth effect at state point 1 is withdrawn by the compressor to raise its saturation pressure and

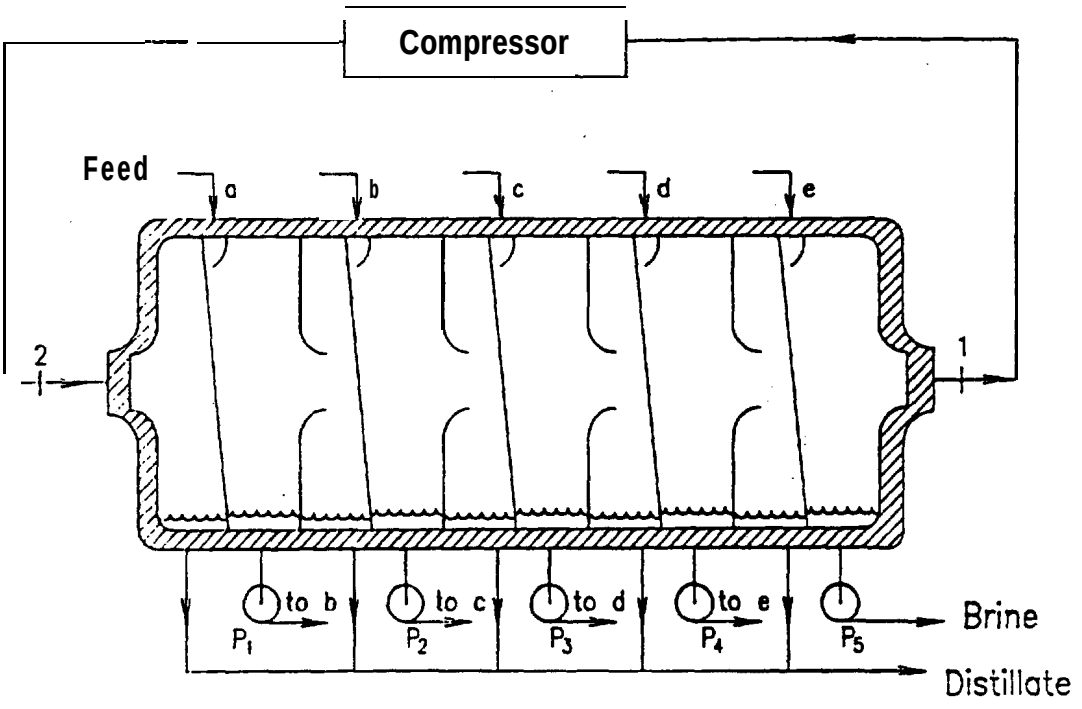

Figure 3 Five effect **vapor** compression system schematic diagram.

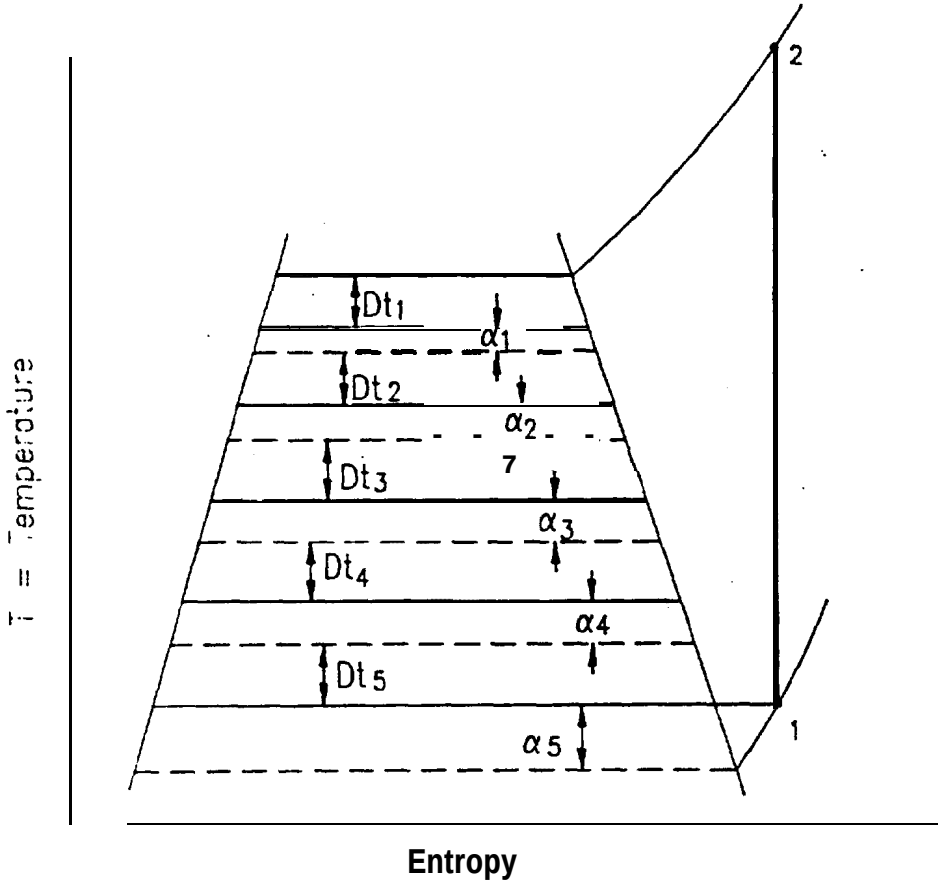

Figure 4. Temperature – Entropy diagram for the five effect vapor compression distillation system corresponding **Lo the** process shown in figure 3.

temperature to state point 2 and is then used as the heating vapor in the first effect. The condensate streams from the five effects are manifolded and taken out as product. The work required by the compressor to compress the vapor from state point 1 to state point 2 must overcome the effects of dissolved solids in each of the five effects ($\alpha_1, \alpha_2, \alpha_3, \alpha_4, \alpha_5$) as well as supply the sum of the temperature difference Dt required in each of the five effects. The isentropic compression work required to compress one kg of vapor from state point 1 to state point 2 is given by:

$$W_5 = C_p T \, [\mathrm{Exp} \, \{\Gamma(\Sigma Dt + \Sigma\alpha)/C_p T^2\} - 1] \qquad (6)$$

here W_5 is the work required to compress one kg of vapor, however, the unit will produce about 5 kgs of distillate for each kg of vapor compressed by the compressor. Therefore, the isentropic work required by the unit per kg of distillate from the plant is approximately one fifth of that shown in Eq. 6. It should be noted here that for a conventional SEVCD unit and a five effect VCD unit operating at the same temperature difference Dt, the value of $\Sigma\alpha$ in Eq. 6 is less than the value of 5α in Eq. 4 due to the progressive increase of salinity in each of the effects in comparison to conventional SEVCD units. This fact implies that the work required per unit of product from the five effect VCD unit is less than that from a conventional SEVCD unit for the same value of Dt regardless of the type of evaporator.

As an example assume a situation in which it is desired to recover 95 percent of the water from a 10,000 ppm salt solution in a VCD unit operating at an average temperature of 50° C. For simplicity and availability of data on sea salt solutions (6), the feed is assumed to have seawater composition. Figure 5 shows the ratio of the isentropic work W_n required by a MEVCD per unit of product from the plant to that of a SEVCD as a function of Dt for three conditions; 2 effects, 5 effects, and 10 effects VCD. In this figure Dt is assumed to be the same in all the effects and that each effect produces the same amount of distillate. In a S-effect system operating at the above conditions the calculated salinity and corresponding boiling point elevation in each effect are respectively; S_1 = 12346 ppm, α_1 = 0.128" C, S_2 = 16129 ppm, α_2 = 0.169" C; S_3 = 23256 ppm, α_3 = 0.249" C; S_4 = 41667 ppm, α_4 = 0.469" C; S_5 = 200,000 ppm, α_5 = 3.198". C. For a value of Dt = 1° C, the values of W and W,, calculated from Eqs. 4 and 6 are respectively, 32.20 and 74.63 kJ/kg, however, for each kg of vapor compressed by the compressor in a 5-effect system the plant produces 5 kg of product, and thus the energy required per unit of product from the 5-effect plant is 14.93 kJ/kg and the ratio W_n/W per unit of product is 14.93/32.20 = 0.46, which corresponds to the value shown on Fig. 5. Figure 5 shows that the use of two effects results in significant saving of energy (lower ratio). It is also of interest to note that the use of 10 effects results in negligible saving as compared to the use of 5 effects. Obviously, the optimum number of effects will depend on compressor type, type of feed, and other parameters that are beyond the scope of this program.

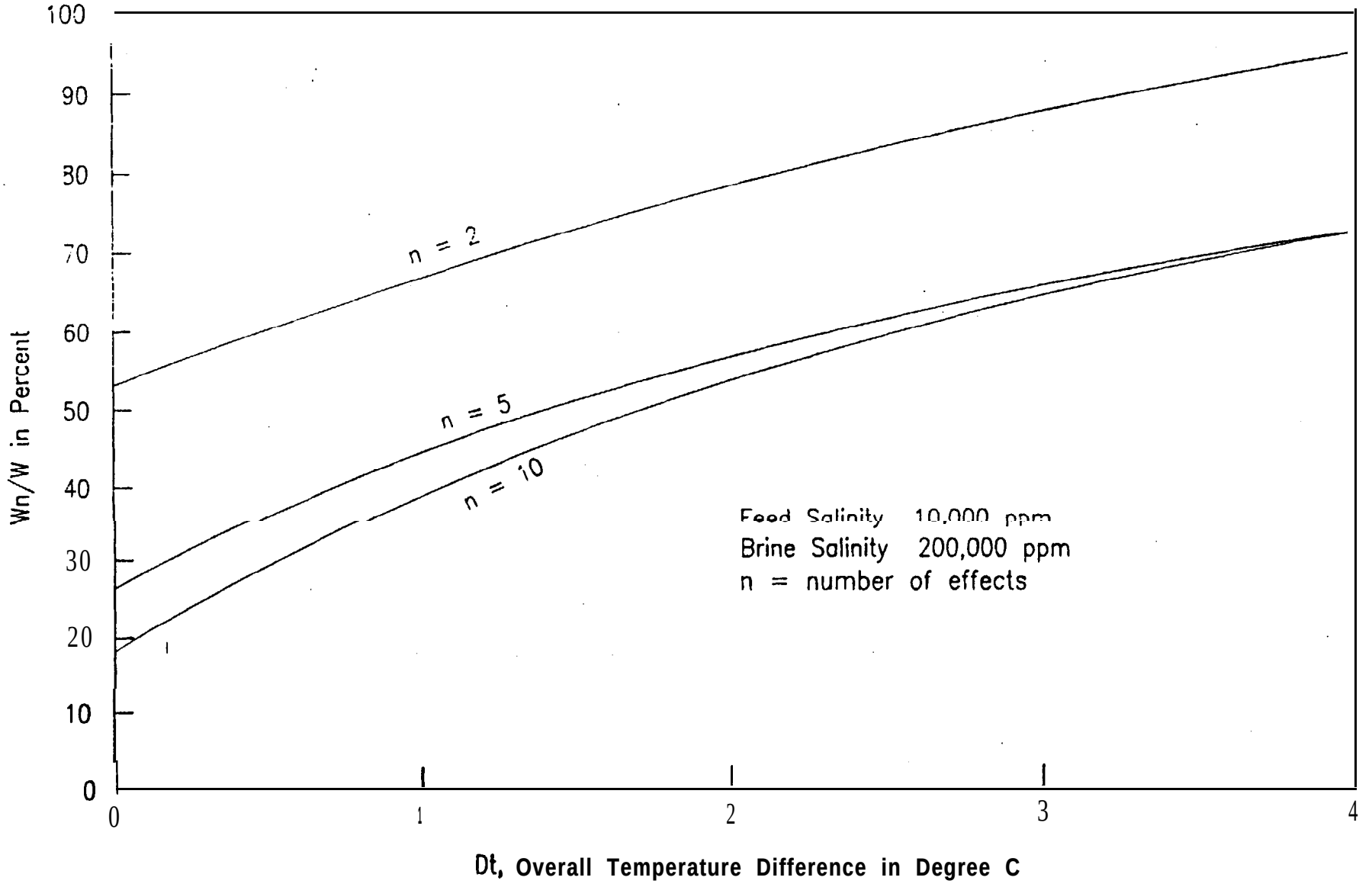

Figure 5. Ratio of isentropic energy consuniption per unit of product by multieffect' VCD to single effect VCD as a function of overall temperature difference across the heat transfer surface for an average evaporator temperature of 50°C

The Wiped Film Rotating Disk Evaporator

Figure 6 is a schematic cross section of the evaporator. Fig. 7 is a schematic cross section taken between two disk pairs. Fig. 8 is a cross section of the wiper taken between the inside and outside periphery of the disk showing the relative position of the wiper and disk. The rotor consists of disk pairs joined together at the outside periphery of the disks. Although Fig. 6 shows only four disks forming two cavities, the rotor in each effect of the existing five effect unit contains 10 disks forming five cavities. The rotor is mounted on a stationary shaft closed at one end and open at the other end. Steam from a boiler, from a previous effect, or from a compressor, is introduced into the open end of the shaft and is condensed on the inside surfaces of the disks. The condensate is thrown by centrifugal force to the periphery where it enters stationary product tubes (scoops) connected to a central tube, and flows out of the evaporator as distillate product. The rotor rotates inside a chamber into which the aqueous solution is fed along the length of stationary wipers (Figs. 7 and 8), where it is deposited as a thin, uniform film on the outside surfaces of the rotating disks in a manner that prevents the formation of dry spots. Unevaporated feed is slung from the periphery of the disks onto the inside walls of the chamber where it is withdrawn from the bottom of the chamber as blowdown (residue). The combination of centrifugal force and wiped feeding achieves a thinning of both condensate and feed films which result in exceptionally rapid heat transfer.

Experimental Apparatus

Figure 9 shows the flow diagram of the existing five effect VCD unit. In this unit effects 1 and 2 have one circulating pump and effects 3 and 4 also have one circulating pump while effect 5 has its own circulating pump. The feed is preheated in the distillate and brine coolers by cooling the distillate and brine streams and then enters the first effect. The unevaporated parts of the solutions from the first and second effect are withdrawn by circulating pump 1. This stream *is* circulated back to these two effects and supplies the feed to the third effect through asolenoid valve. Similarly the unevaporated parts of the solutions from the third and fourth effects are withdrawn by circulating pump 2. This stream is circulated back to these two effects and supplies the feed to the fifth effect through another solenoid valve. The unevaporated portion of this solution in the fifth effect is circulated back to this effect and a portion of it is withdrawn by a positive displacement pump and discharged as concentrated blowdown. The blowdown is cooled in the brine cooler prior to being discharged back into the feed storage tank. The condensate from the five effects is collected in a condensate sump where the distillate is pumped through the distillate cooler and then discharged back into the feed storage tank.

The vapor generated in the first effect is used as the heating vapor in the second effect. This process is repeated in effects 2, 3, and 4. The vapor generated

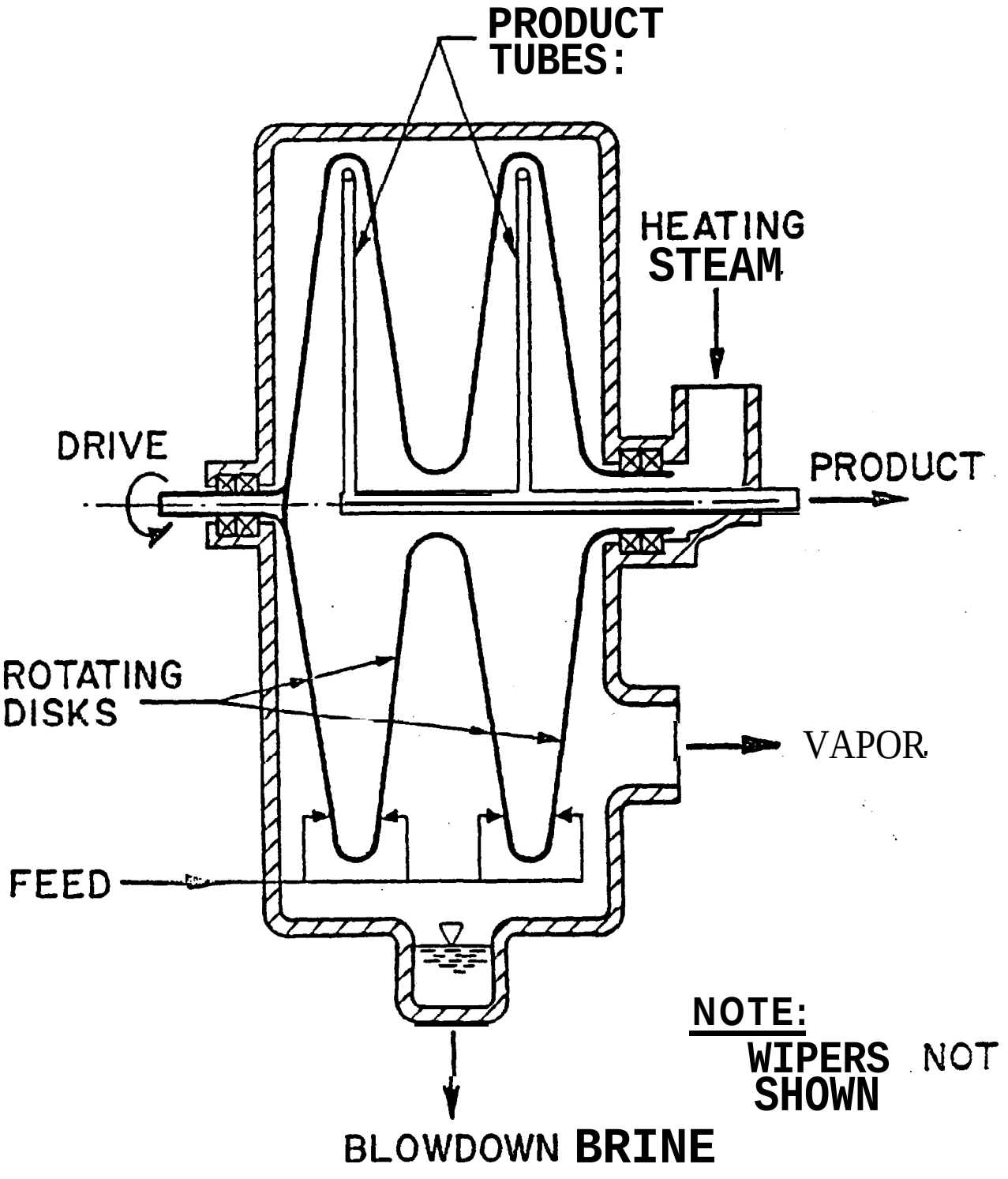

FIG. 6 ROTATING-DISK WIPED-FILM EVAPORATOR CROSS SECTION "SCHEMATIC"

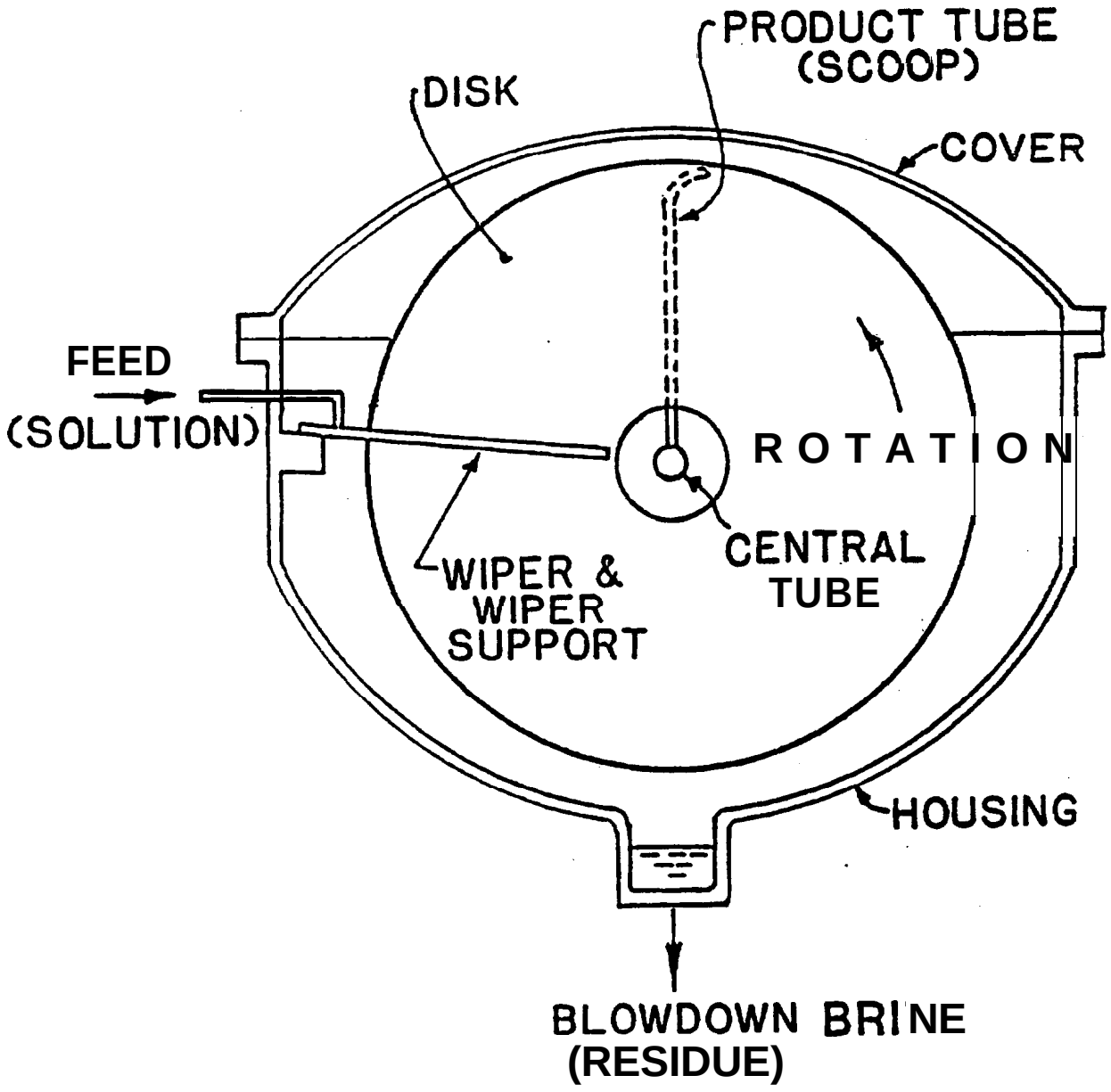

FIG. 7 EVAPORATOR CROSS SECTION BETWEEN DISK PAIRS OF FIG. 6 "SCHEMATIC"

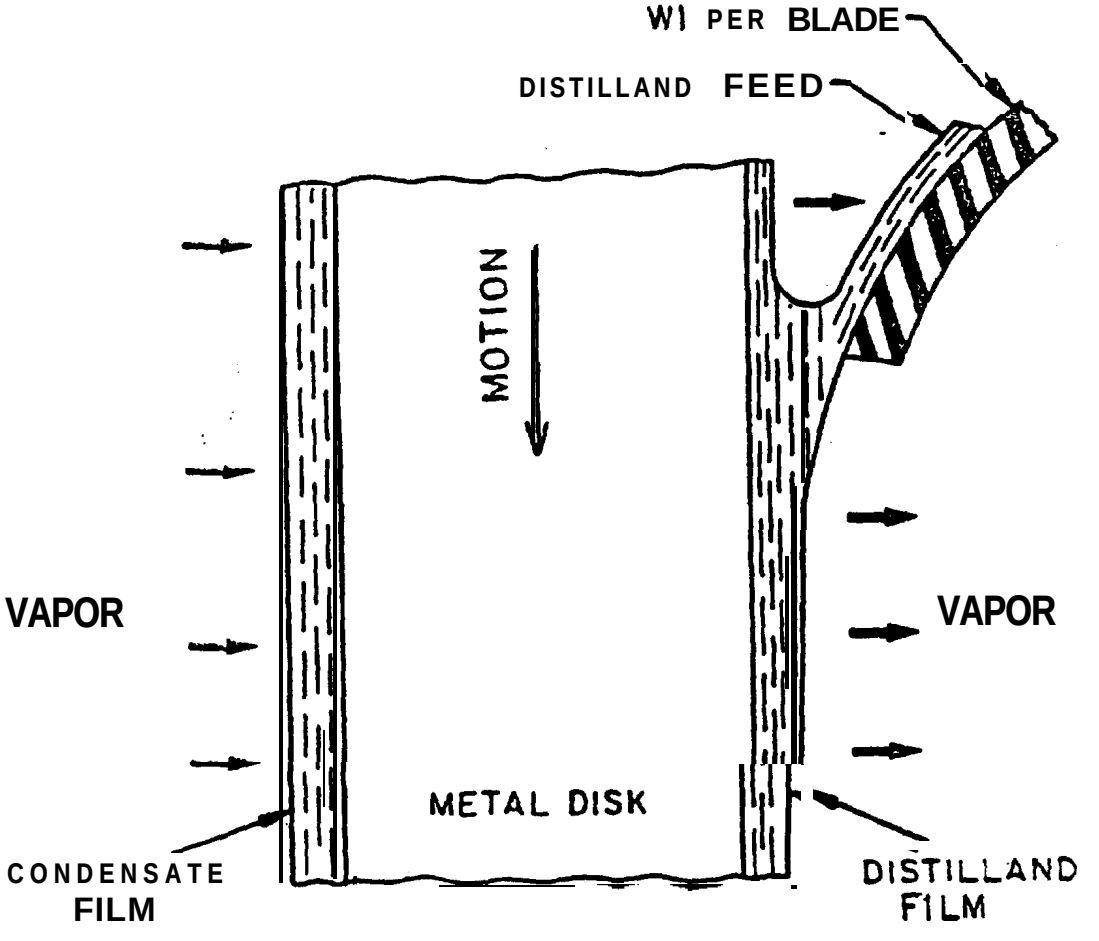

FIG. 8 CROSS SECTION OF THE WIPER BLADE AND METAL DISK IN A TANGENTIAL DIRECTION

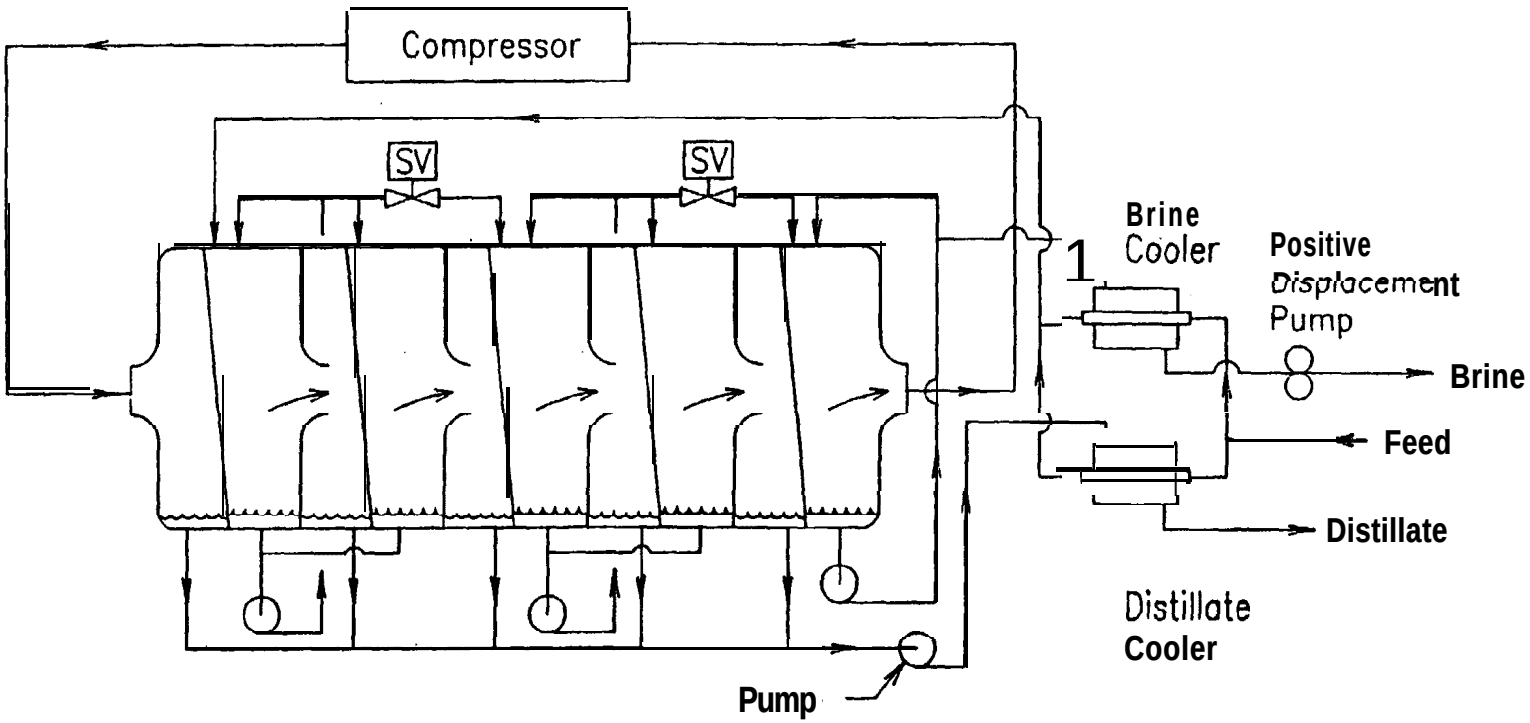

Figure 9. Schematic diagram of existing five effect VCD unit.

in the fifth effect is compressed by a lobe type positive displacement co' .r essor and is then used as the heating vapor in the first effect.

Test Program

Data were collected to determine energy consumption by compressor, energy consumption by rotor, brine salinity, individual overall heat transfer for each effect, and the average overall heat transfer coefficient for the unit. The simulant feed solution was made up by collecting'about 1130 liters (300 gallons) of distilled water and dissolving in it 8.62 kg (19 lbs) of sodium sulfate and 2.' 7 kg (6 Ibs) of sodium chloride. The resulting solution has a salinity of about 10,00 ppm consisting of 5160 ppm sulfate, 1460 ppm chloride, and 3380 ppm sodium. Table I shows. the composition of agricultural drainage water in the San .is drain at Los Banos, California and the composition of the simulant solution

The energy consumption by the compressor and cs drive was determined by measuring the power input to the compressor motor divided by the distillate rate. The power was measured by a laboratory type t neter. Similarly, the energy required to drive the rotors was determined by measuring the power input to the rotors motor divided by the distillate rate. The brine salinity was determined by salt balance. This was done by measuring the condensate mass rate and brine blowdown mass rate and assuming that the feed mass rate is equal to the sum of the distillate mass rate and brine blowdown mass rate. The mass rate of the distillate was determined by measuring the time required to fill a calibrated Volume. The brine mass rate was determined by measuring the time required to fill a calibrated. 100 ml flask and then weighing this flask. The brine salinity was determined by salt balance and was calculated by the equation:

$$S_b = S_f(m_b + m_d)/m_b \qquad (7)$$

Because brine blowdown mass rate was determined by measurements, it was used to calculate brine blowdown salinity in the fifth effect using Eq. 7. As a comparison, the brine salinity, brine density, and boiling point elevation
were calculated from the chemical composition of the brine using relations given by Fabuss (6). The calculated values of the salinity from these relations were consistently lower than the values calculated by salt balance using Eq. 7. This fact. suggests that calculated values of the boiling point elevation may be lower than actual values.

The overall heat transfer coefficient was calculated from the following relation:

$$U = m_d r/A\ Dt \qquad (8)$$

The temperature at 11 locations in the unit was measured by 11 calibrated platinum

TABLE I

Agricultural Water Analysis: Sample taken on October 13, 1982 from San Luis Drain at Desalting Site, Los Banos, California
Analysis made by DWR

Element	mu/liter
Sodium	2160
Calcium	500
Magnesium	264
Potassium	6.9
Sulfate	4610
Chloride	1440
Boron	16
Silica as SiO_2	20
Total alkalinity as $CaCO_3$	169
Total Hardness as $CaCO_3$	2340
Specific conductance at 25° C	11300micromhos/cm
pH	8.1
Total Dissolved Solids	9370

Composition of Simulant Solution

Element	ma/liter
Sulphate	5160
Chloride	1460
Sodium	3380
Total Dissolved Solids	10000

resistance temperature detectors (RTD). These 11 RTD's were located as follows; one in the vapor space in each of the five effects, one in the vapor space of the condensate stream in each of the five effects, and one located at the outlet of the compressor.

Data and Results

Table II shows the tabulated data obtained from the simulant solution for 47 runs. Column 1 shows the evaporator temperature, t_5, in the fifth effect. Column 2 shows the average temperature drop, Dt, across each effect which was calculated by adding the measured temperature drop across each of the five effects and dividing the result by 5. Column 3 shows the average overall heat transfer coefficient, U, for the unit. Column 4 shows the brine blowdown salinity S_b calculated from salt balance (Eq. 7). Column 5 shows the brine blowdown salinity S_d calculated using measured brine blowdown density and the composition of the brine using the relations given by Fabuss. Column 6 shows the boiling point elevation, a, of the brine (blowdown brine) in the fifth effect using the salinity shown in Column 4 and the relations given by Fabuss. Column 7 shows the sum of the boiling point elevations $\Sigma\alpha$, in the five effects calculated in a similar manner to that used in calculating a in the fifth effect. Column 8 shows the specific isentropic energy consumption, E,, calculated from Eq. 1 using the measured pressure in the fifth effect and pressure rise across the compressor. The pressure in the fifth effect was measured by an absolute mercury manometer and the pressure rise across the compressor was measured by a water manometer. Column 9 shows the measured specific energy input to the compressor motor, E,. Column 10 shows the measured specific energy input to the rotor motor, E_r. Column 11 shows the sum of Column 9 and 10 and shows the total specific energy consumption by the compressor and rotors motors. Column 12 shows the condensate flux which was calculated by measuring the condensate rate and dividing this value by the total heat transfer surface area in the evaporator. Column 13 shows the recovery ratio in percent and was calculated as the ratio of distillate mass rate to the sum of the distillate and brine blowdown mass rates.

Figure 10 shows a plot of the value of U using distilled water feed for the individual effects as a function of the overall temperature difference Dt across the heat transfer surface in that effect for three temperatures, 100° F, 110" F, and 120° F. The values of U were calculated by assuming that the mass rate of the condensate in each effect to be equal to one fifth of the measured condensate mass rate from the unit. The two lines show the predicted value of U for 90° F and 130° F using Eqs. 16 and 17 from Reference 6 for clean heat transfer surfaces using properties of water at these two temperatures. It is significant to note here the effect of operating temperature on U, the lower the operating temperature the lower the value of U. This is to be expected since lower temperature results in higher fluid viscosity and lower thermal conductivity of water. The higher viscosity results in thicker

Table II

Data and Results from the Simulant Solution

t_5 °F	Dt °F	U a	S_b b	S_d b	a °F	$\Sigma\alpha$ °F	E_{is} c	E_c c	E_r c	E_t c	F d	Rec. %
119	2.10	2602	207	180	2.73	4.16	14.2	32.1	19.9	52.0	4.73	95.2
120	2.22	2413	194	168	2.58	3.99	14.5	31.5	20.3	51.8	4.78	94.9
121	2.12	2579	164	146	2.20	3.57	14.2	30.7	19.3	50.0	5.04	93.9
119	2.13	2553	188	•	2.50	3.91	12.6	27.9	19.4	47.3	4.98	94.7
122	2.11	2629	166	154	2.23	3.61	13.8	30.5	18.7	49.2	5.04	94.0
122	2.09	2575	171	160	2.28	3.67	14.0	32.0	18.9	50.9	4.97	94.1
121	2.04	2629	172	157	2.30	3.69	13.7	31.5	18.7	50.2	4.98	94.2
121	2.08	2753	186	152	2.47	3.88	13.7	29.2	18.1	47.3	5.34	94.6
121	2.12	2627	177	156	2.36	3.75	14.0	31.1	18.4	49.5	5.09	94.3
120	2.03	2653	166	158	2.22	3.60	14.0	30.4	18.5	48.9	4.93	94.0
121	2.04	2710	172	152	2.30	3.68	13.9	31.1	18.1	49.2	5.05	94.2
98	1.37	2257	128	104	1.73	3.04	11.2	26.8	29.9	56.7	2.87	92.2
111	1.62	2651	156	130	2.10	3.46	12.5	27.6	22.7	50.3	4.01	93.6
118	2.05	2578	171	127	2.28	3.67	12.5	29.1	19.5	48.6	4.83	94.1
118	1.88	2711	164	137	2.20	3.58	13.1	29.3	20.0	49.3	4.70	93.9
116	1.91	2614	158	145	2.12	3.48	12.5	29.4	20.6	50.0	4.54	93.7
119	1.95	2627	173	145	2.32	3.70	13.2	29.7	19.6	49.3	4.7s	94.2
117	2.01	2475	173	149	2.31	3.70	12.9	29.2	19.9	49.1	4.60	94.2
86	0.88	2389	150	34	2.02	3.37	9.2	28.9	42.0	70.9	1.96	93.3
97	1.36	2218	166	131	2.23	3.61	11.4	26.3	29.5	55.8	2.80	94.0
106	1.49	2512	180	155	2.40	3.80	12.8	26.1	24.5	SO.6	3.43	94.5
110	1.52	2747	165	171	2.21	3.59	12.2	26.6	21.9	48.5	3.84	93.9
109	1.58	2687	169	149	2.27	3.65	12.1	26.2	21.8	48.0	3.88	94.1
109	1.62	2594	169	139	2.26	3.64	11.9	26.6	22.1	48.7	3.83	94.1
109	1.70	2461	178	152	2.38	3.78	12.4	26.8	21.6	48.4	3.84	94.4
109	1.64	2576	179	157	2.39	3.78	12.4	26.1	21.9	48.0	3.85	94.4
110	1.68	2523	177	159	2.36	3.75	12.6	25.8	21.6	47.4	3.85	94.3
110	1.60	2589	174	160	2.32	3.71	12.2	25.6	21.8	47.4	3.85	94.2
106	1.45	2565	143	126	1.92	3.26	11.5	25.4	24.2	49.6	3.54	93.0
106	1.65	2305	340	141	1.89	3.22	11.1	26.1	24.4	50.5	3.52	92.8
106	1.53	2464	142	132	1.91	3.25	11.1	25.7	23.6	49.3	3.56	92.9
106	1.39	2745	142	125	1.92	3.25	11.1	25.3	23.1	48.4	3.58	93.0
116	1.53	2486	142	126	1.91	3.25	11.6	25.8	23.2	49.1	3.54	93.0.
85	0.91	2221	141	41	1.90	3.24	12.8	28.6	43.2	71.8	1.90	92.9
93	1.17	2308	154	105	2.07	3.43	10.9	27.0	32.6	59.6	2.54	93.5
105	1.51	2475	156	146	2.10	3.46	11.3	25.0	24.4	49.4	3.51	93.6
106	1.44	2440	129	104	1.75	3.06	11.4	28.1	26.7	54.8	3.33	92.3
106	1.57	2443	140	187	1.89	3.22	11.4	26.4	23.9	so.3	3.59	92.9
107	1.42	2501	140	136	1.89	3.22	31.1	26.8	25.6	52.4	3.38	92.9
116	1.68	2508	144	124	1.93	3.28	11.3	25.7	24.4	50.1	3.51	93.0
96	1.12	2337	155	93	2.09	3.45	9.1	26.8	32.0	58.8	2.59	93.6
103	1.46	2275	151	148	2.03	3.39	12.2	29.1	27.7	56.8	3.01	93.4
108	1.75	2222	166	150	2.22	3.60	13.6	27.9	24.2	52.1	3.57	94.0
113	1.75	2423	127	149	1.72	3.03	12.5	29.8	23.4	53.2	3.80	92.1
119	1.93	2516	143	136	1.93	3.27	14.1	31.1	20.9	52.0	4.46	93.0
122	2.21	2734	171	121	2.29	3.67	14.1	26.2	16.9	43.1	5.61	94.1
122	2.18	2544	149	101	2.01	3.36	14.0	28.1	19.1	47.2	5.26	93.3

a: Btu/hrft^2°F; b: parts/1000; c: kWhr/ kgal; d: lbs/hrft^2

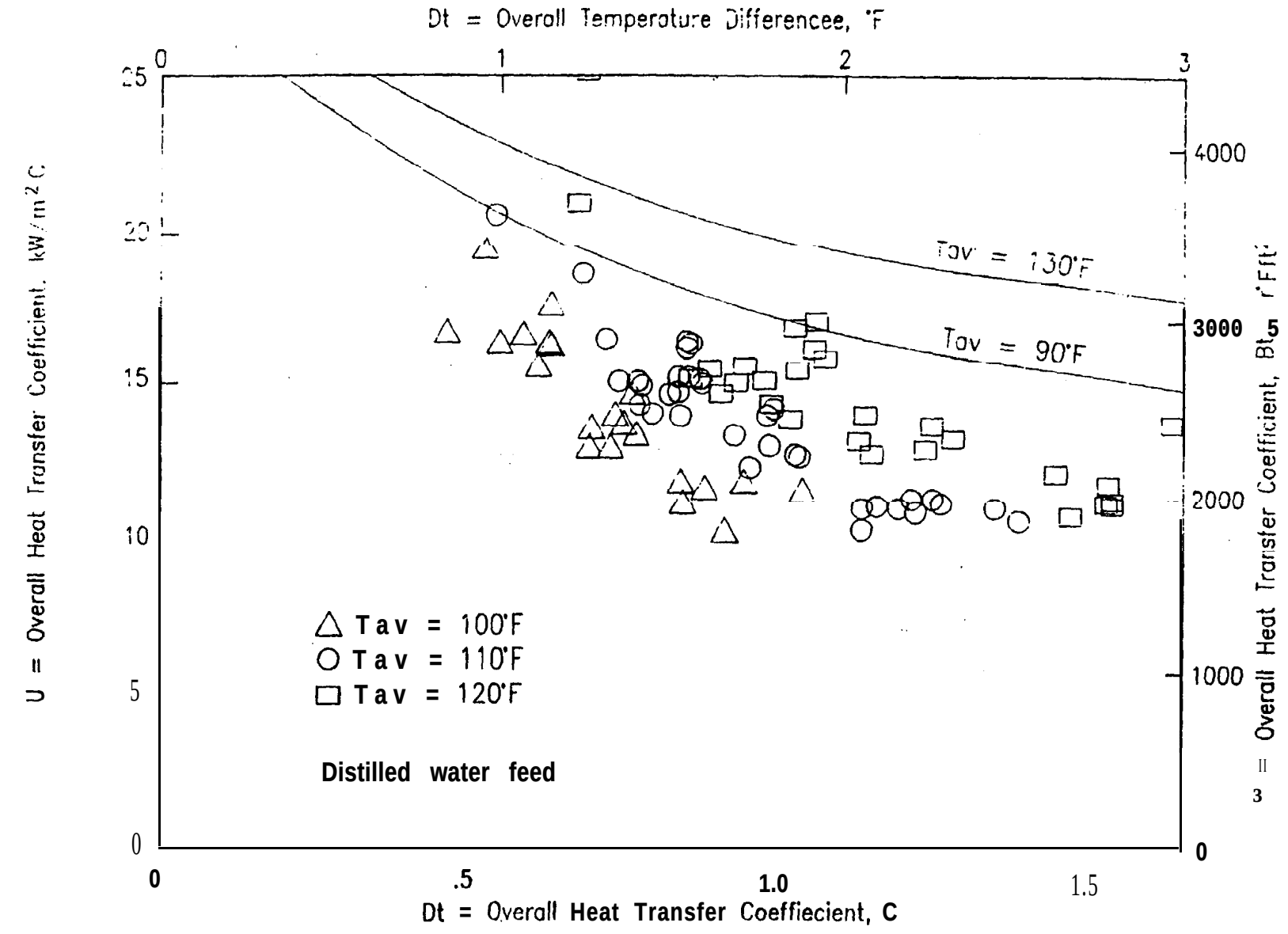

Figure 10. Overall heat transfer coefficient of individual effects as a function of overall temperature difference for the temperatures shown.

condensate and feed films on the disks while lower thermal conductivity results in high resistance to the flow of heat, the consequences' of which result in lower values of U. Thus, at constant Dt, the value of U will increase as operating temperature in the evaporator increases.

Figure 11 shows a plot of the value of U for the individual effects as a function of Dt for the simulant solution for three temperatures; 100° F, 110° F, and 120° F. The value of U was calculated in a similar manner to that used for distilled water. The effects of salinity on the value of U was slight in the first four effects due to the relatively low brine salinity in the first four effects, however, the value of U was significantly lower in the last effect due to high brine salinity (150,000 to 200,000 ppm) due to higher viscosity and lower thermal conductivity of the brine. The two lines for 90° F and 130° F are the same as those shown on Fig. 10. Again, the same trend shown on Fig. 10, namely the dependence of U on evaporator temperature, is also shown for the brine on Fig. 11.

Figure 12 shows a plot of the average value of U for the evaporator as a function of the average Dt across the five effects for the temperatures shown on the figure. The average value for these data was about 14 kW/m^2 ° C (2500 $Btu/hrft^2$ ° F) at an overall temperature difference ranging from 0.35" C at the low temperature end (32" C) to about 1.25° C at the high temperature end (60° C). The trend here reflects the same trend shown on Figs. 10 and 11, namely the dependence of U on temperature.

Figure 13 shows a plot of the specific energy consumption by the rotors and compressor as a function of distillate flux. The lower line shows the specific energy consumption by the rotors alone while the upper data show the sum of the specific energy consumption by the compressor and rotors. It is significant to note the dependence of energy consumption by the rotors on flux, the lower the flux the higher the energy consumption. This is because the energy consumed by the rotors is due to friction in the bearings of the rotors and drive shaft as well as the energy imparted to the feed and condensate to acquire the velocity at the outside rim of the disks. These values are relatively constant regardless of the value of the flux. Thus, when the product rate increases, the flux increases resulting in lower specific energy consumption by the rotors as shown in the figure. At design values of 37 $kg/hr\ m^2$ (7.5 $lbs/hrft^2$) the specific energy consumption by these particular rotors is expected to-be about 3 $kWhr/m^3$ (12 kWhr/kgal) or less.

Discussion

The data presented in our third progress report (appendix A) were obtained from the 40 gal/hr NASA unit using distilled water feed. The data obtained with the simulant solution were obtained from the 100 gal/hr unit. The NASA unit has heat transfer disks made from 0.024 inch thick type 316 stainless steel sheets. The 100

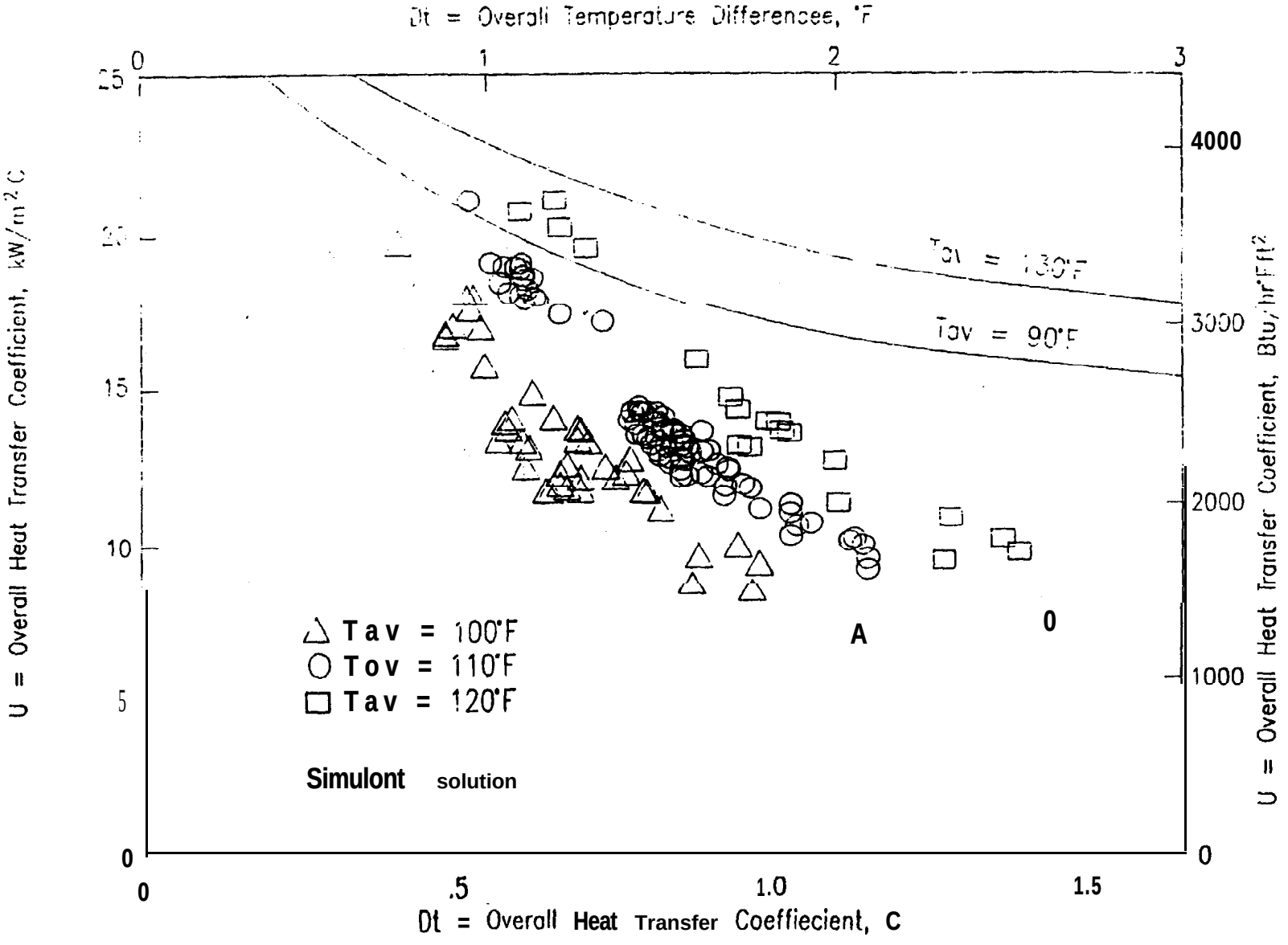

Figure 11. Overall heat transfer coefficient of individual effects as a function of overall temperature difference for the temperatures shown.

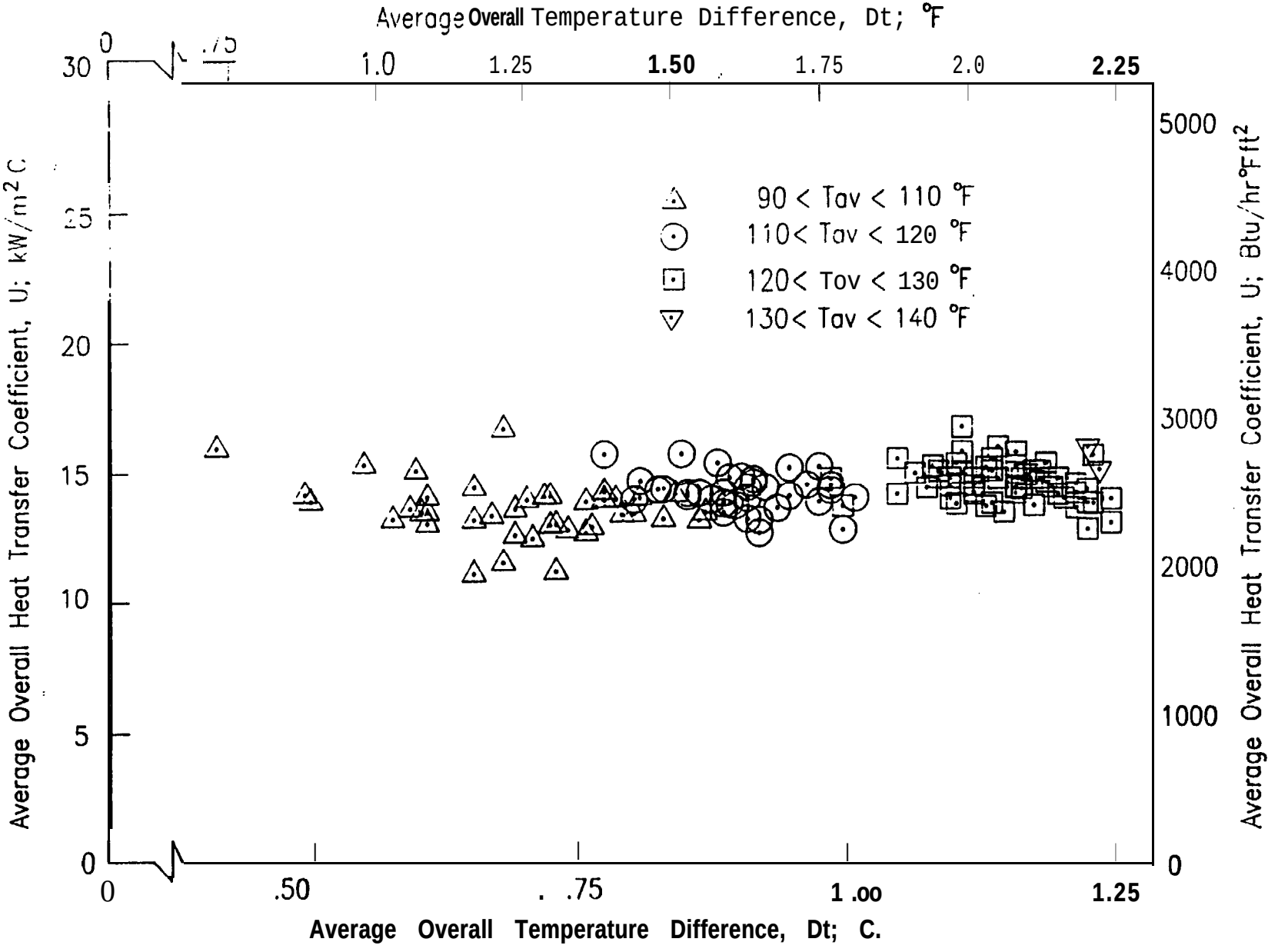

Figure 12. Average overall heat transfer coefficient as a function of the average overall temperature difference for the temperature range of 32 to GO C.

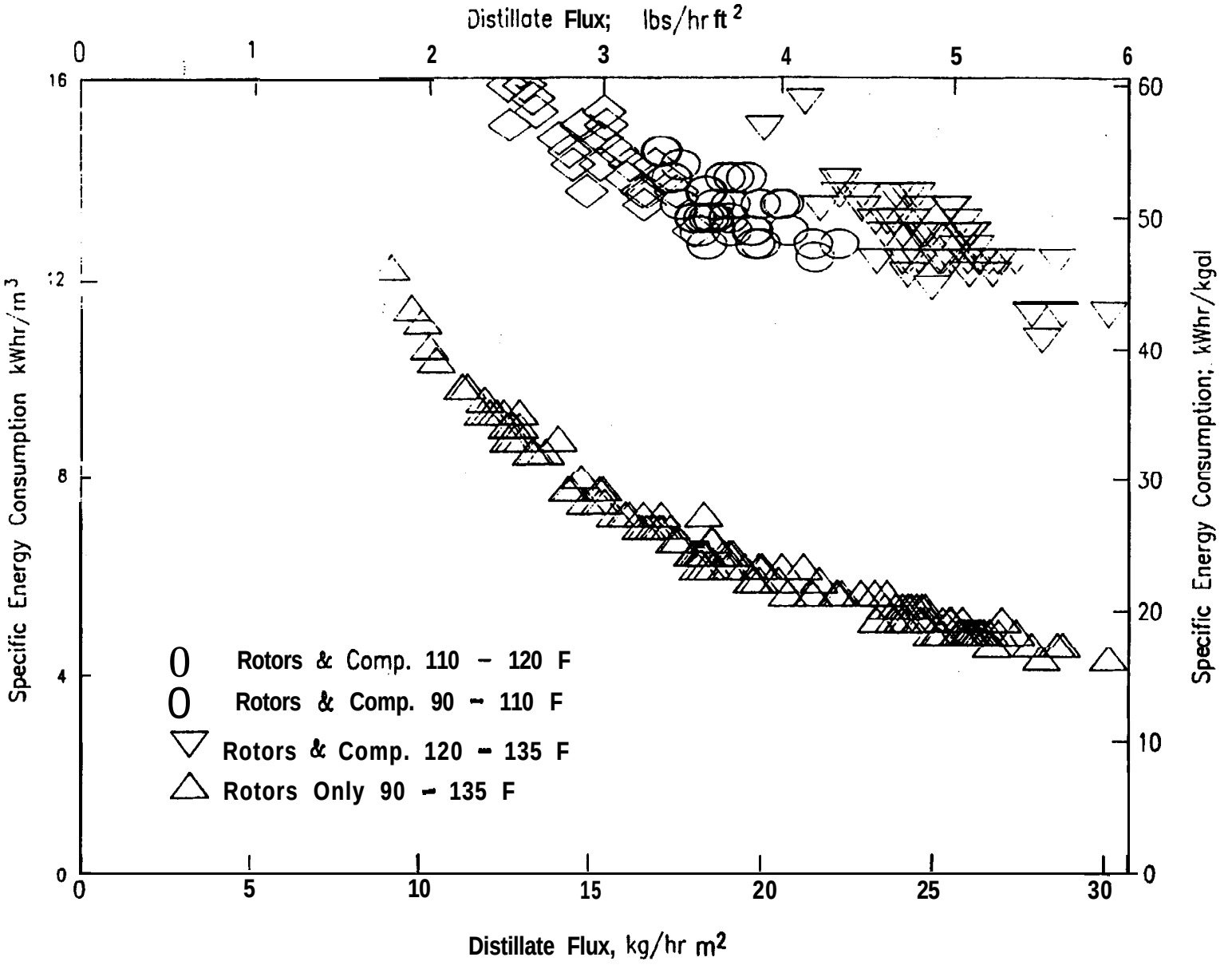

Figure 13. Specific energy consumption by the rotors and by the rotors and compressor as a function of distillate flux.

gal/hr unit has heat transfer disks made from 0.035 inch thick copper sheets. The data obtained from the NASA unit resulted in values of U that were in agreement with analytical predictions (7). The data obtained from the 100 gal/hr unit during this test resulted in values of U that were lower than values predicted analytically. However, the first set of data obtained from the 100 gal/hr unit (when new) using tap water (8) resulted in values of U that were in excellent agreement with analytical predictions. This unit is about seven years old now. It has been used sporadically. The heat transfer surfaces were open to the atmosphere most of the time during shutdown. This caused the copper disks to be oxidized on the condensation side. Testing of this unit with tap water and with 5000 ppm tap water sodium chloride solution caused a very thin layer of calcium carbonate scale to be deposited on the evaporation side of the rotors in the last two effects. No effort was made to remove this scale from the surfaces of the disks prior to obtaining these data. In addition, the high concentration of the brine in the last two effects also added additional resistance to heat flow across the brine film due to increasing viscosity and decreasing thermal conductivity of the brine. We believe these factors caused the values of U (an average of 14.2 $kW/^{\circ}$ Cm' ; 2500 $Btu/^{\circ}$ $Fhrft^2$) to be little lower than prediction. The values of U obtained during this test are about ten times higher than the values obtained from a 50,000 gal/day vapor compression evaporator tested at Los Banos using agricultural drainage water with hexametaphosphate additive for scale prevention (1) .

The compressor in this unit is a lobe type positive displacement compressor. Its volumetric capacity is directly proportional to speed and somewhat inversely proportional to pressure rise due to vapor back leakage in the clearances between the housing and lobes. The energy input to the compressor motor consists of energy loss in the electric motor, energy loss in drive belts, energy loss in friction in the bearings, seals, gears, and energy imparted to the vapor. The lower the operating temperature, the higher these losses in comparison to the energy imparted to the water vapor during compression. For example, in one of the runs, the vapor inlet temperature (temperature in the fifth effect) was about 86° F (see Table II). The, measured flux was 8.6 kg/hrm^2 (1.96 $lbs/hrft^2$) and the measured energy' consumption, E_c, was 7.64 $kWhr/m^3$ (28.9 kWhr/kgal) while the calculated value of E_{is} was 2.43 $kWhr/m^3$ (9.2 kWhr/kgal) resulting in isentropic efficiency of 31.8%. As a comparison in one of the runs at 50° C (122" F), the measured flux was 245 kg/hrm^2 (5.61 $lbs/hrft^2$) and the measured energy consumption, E_c, was 6.92 $kWhr/m^3$ (26.2 kWhr/kgal) while the calculated value of E_{is} was 3.73 $kWhr/m^3$ (14.1 kWhr/kgal) resulting in isentropic efficiency of 53.8%. Unfortunately, due to the high salinity of the brine in the last effect, the pressure rise across the compressor at temperatures higher than 50° C (122° F) in the fifth effect was beyond the capacity of our water manometer, thus no data were collected close to the design flux value of 32.7 kg/hrm^2 (7.5 $lbs/hrft^2$). We believe that at the design flux of 32.7 kg/hrm^2 (7.5 $lbs/hrft^2$), the compressor isentropic efficiency could be 60% or better.

Column 11 and Fig. 13 show the total specific energy consumption by the compressor and rotor, E,. This value ranged from a value of 11.4 $kWhr/m^3$ (43.1

kWhr/kgal) at a flux of 24.5 kg/hrm^2 (5.61 lbs/hrft^2) to as high as 19.0 kWhr/m^3 (71.8 kWhr/kgal) at a flux of 8.3 kg/hrm^2 (1.90 lbs/hrft^2). It can be seen here that the value of E_t was about 13.2 kWhr/m^3 (50 kWhr/kgal) and lower when tbe flux was higher than 17.5 kg/hrm^2 (4 lbs/hrft^2). This is due to the fact that energy consumption by the rotors increases very slightly as the flux increases due to the higher condensate rate, however, the specific energy consumed by the rotors, E_r, decreases with increasing flux, as shown in Fig. 12. Therefore, with improved rotor design and at a design flux of 32.7 kg/hrm^2 (75 lbs/hrft^2) we believe that specific energy consumption by the rotors could be 2.64 kWhr/m^3 (10 kWhr/kgal) or less and the total specific energy consumption by the compressor and rotors could be 10.6 kWhr/m^3 (40 kWhr/kgal) or less for this application. This figure is less than half the energy consumed by the compressor in the 50,000 gal/day vapor compression unit tested at Los Banos (1).

The application of these results to coupling this type of evaporator in multieffect configuration to salt gradient solar ponds will result in more efficient energy use of the energy extracted from the solar ponds. As an example assume that we like to use this type of evaporator configured in multieffect mode coupled to a salt gradient solar pond whose bottom convecting layer is at an average temperature of 65" C and top convecting layer at an average temperature of 20° C and would like to know the amount of distillate produced from the multieffect plant per unit energy extracted from the pond. Here we propose the following:

1. Extract brine from the bottom layer of the pond, flash it in a vacuum chamber to generate water vapor at about 57" C (8" C flashdown) with this vapor fed into the first effect and the brine returned to the bottom of the pond.

2. Feed water enters the final condenser to condense the water vapor from last effect and is heated from 20° C to 28° C.

3. Approach temperature in the final condenser is 3" C.

4. Average overall heat transfer coefficient, U = 14 kW/° Cm^2.

5. Feed salinity 10,000 ppm and brine salinity at 200,000 ppm resulting in an average boiling point elevation of about 0.35" C.

At these conditions, the temperature drop available to the multiple effect system is calculated to be about 26" C. For a flux of 27 kg/hrm^2 and U = 12 kW/° Cm^2, the required Dt per effect is 1.76" C. Therefore, the number of effects that can be installed is about 12. The total production from the plant including the condensate from the first effect and final condenser is estimated to be about 11 kg per kg of steam generated from the solar pond or a performance ratio of about 11. Thus, 'for each 1 kWhr of thermal energy extracted from the solar pond, it is possible to produce about 37 kg of water from this type of distillation plant. Assuming the

collection efficiency of the solar pond at this temperature is about 15%, the total incident solar energy of 5 $kWhr/m^2$ day, the productivity of this type of plant is estimated to be about 28 kg per square meter of solar pond area. As a comparison, the average daily productivity of simple solar stills does not exceed 3 kg. Thus, the coupling of this type of evaporator to solar ponds can produce as much as ten times the amount of water in comparison to simple solar stills.

Conclusions and Recommendations

The data and results from these tests lead to the following conclusions:

1. The use of multieffect VCD reduces. specific energy consumption 'by the compressor by 20 to 50 percent depending on the number of effects,

2. The use of WFRD evaporators gives very high values of overall heat transfer coefficient of 12 to 18 $kW/^{\circ} Cm^2$ at the low temperature of 30° C to 55° C,

3. The total specific energy consumption by the compressor and rotors could be below 11 $kWhr/m^3$ at design flux value of 38 kg/hrm^2,

4. Recovery of 95 percent of the feed as good quality distilled water is easily accomplished,

5. The coupling of WFRD evaporators to salt gradient solar ponds can produce as much as 28 kg/m^2 of solar ponds in comparison to about 3 kg/m^2 of simple solar stills.

Based on the above conclusions we recommend the following:

1. Assessing the potential of multieffect VCD using WFRD evaporators in reducing the volume of the reject brine from the Yuma plant by testing this 5 effect module using RO brine as feed,

2. Consider coupling the existing 5 effect module to an existing salt gradient solar pond to assess its potential in this application.

REFERENCES

1 Bechtc National, Inc. "Final Report, Field Test of a Vapor Compression Evapo ator at the Demonstration Desalting Facility, Los Banos, California," prepar d for the State of California, Department of Water Resources, Specif ation No. 85-31, Contract No. C-50653, San Francisco, California, Augus 1986.

2 Deukr t jian, G., G.K. Van Vleck, and D.N. Kennedy, "Desalting and the Califo i a State Water Project," State of California Department of Water Resou ces, Sacramento, California, September 1984.

3 Gabb: li, Emilio, "A Thirsty Land" International Desalination & Water Reust quarterly, PP 8-19 November/December 1994, Volume 4/3.

4 Tleim it, B.W., A.D.K. Laird, and E.D. Howe, "Analysis and Cost Prediction of R claiming Agricultural Drainage Water Using Multieffect Vapor-Comp ression Distillation, Final Report on Field Testing of the Wiped-Film Rotating-Disk Evaporator" prepared for the California Department of Water Reso ırces; University of California, Richmond, California; UC/DWR Agre ement B55037, Task Order 84-1, November 1985.

5 Dod ge, B. F., "Chemical Engineering Thermodynamics", McGraw Hill, New Yorl., 1944 p. 133.

6 Fab ıss, B. M., "Properties of Seawater" Appendix 2, 2nd Edition, Part B of Principles of Desalination, Editors K. S. Spiegler and A. D. K. Laird, Academic Press, pp. 359-400, November 1980.

7 Tleimat, B.W., "Performance of a Rotating Flat-Disk Wiped-Film Evaporator," ASME Publication No. 71-HT-37, 1971.

8 Tieimat, B. W. and M. C. Tleimat, "A Novel 2500 GPD S-Effects Wiped-Film Rotating-Disk Vapor-Compression Module; Preliminary Results" International Desalination Association Fourth World Congress on Desalination and Water Reuse, State of Kuwait, November 4-8, 1989

Appendix A

Copy of Progress Report No. 3

WATER REUSE TECHNOLOGY
75 INA COURT
ALAMO, CALIFORNIA 94507
Tel. (510)838-0369, FAX (510)838-0565

Quarterly Progress Report No. 3 July 1 - Sept. 30, 1994

REDUCED ENERGY CONSUMPTION EVAPORATOR FOR USE IN DESALTING IMPAIRED WATERS

Contract Number: 1425-3-CR-81-19560

As stated in our letter of September 13, 1994 to Ms. Mulligan, NASA requested their unit to be delivered; The unit was delivered on September 2, 1994 and our unit was returned to us at the same time. Because our unit was idle for over a year, it was necessary to inspect the unit, clean it, and perform some maintenance on it.

After cleaning and maintenance, data were obtained from the unit using distilled water which was produced from the NASA unit and stored in a 300 gallon storage tank. The data obtained include the temperature in each effect, the energy consumption by the rotor, energy consumption by the compressor, product rate, concentrate blowdown rate, absolute pressure in the last effect, and pressure rise across the compressor.

The enclosed table shows data and results obtained from the unit using distilled water. The first column shows the average temperature in the evaporator, the second column, shows the calculated overall heat transfer coefficient, the third column shows the measured distillate flux (distillate rate per unit area of heat transfer surface), the fourth column shows the specific energy consumption by the rotor, the

fifth column shows the specific energy consumption by the compressor, and the last column shows the sum of columns four and five. The first set of rows were collected using four rotors while the last six rows were collected using all five rotors.

Fig. 1 shows a plot of the calculated overall heat transfer coefficient, U, for each effect as a function of the overall temperature difference, Dt, across the effect for the temperature range of 90 to 140 F. It is significant to note here that the value of U increases when t_{av} increases. This is expected due to the effects of viscosity and thermal conductivity on heat transfer coefficient. As the temperattire rises the thermal conductivity of the water increases and the viscosity of the water decreases resulting in a higher value of U for the same Dt.

Pig. 2 shows a plot of the energy consumption by the rotor as a function of distillate flux. It is significant to note here that the energy consumption decreases with increasing flux. This is due to the fact that the energy consumed by the motor driving the rotors does not change. significantly when the distillate rate increases. Thus, when the average evaporator temperature increases, the specific volume of the vapor from the last effect decreases resulting in a larger mass flow rate through the compressor and, as a consequence, higher distillate flux. It should be noted here that when the fifth rotor was added to the unit, the specific energy consumption decreased for the same flux. It should be pointed out that the unit was designed for flux in excess of 7 and as a consequence E_r would be less than.15 Whr/gal.

Planned Activities for the Fourth Quarter

As stated earlier, the amount of distilled water produced from the NASA unit was stored in a 300 gallon storage tank.

In order to simulate the saline solution of the agricultural drainage water, we mixed 19 pounds of sodium sulfate and six pounds of sodium chloride with approximately 300 gallons of distilled water stored in the tank. The calculated composition is:

Sulfate	5087 ppm
Chloride	1434 ppm
Sodium	3379 ppm

Total salinity = 9900 ppm

This solution is quite similar to the composition of the agricultural drainage water taken from the San Luis Drain as shown 'in our letter of August 6, 1993 to Ms. Mulligan with calcium, magnesium, and silica not being included in'the simulant solution.

Data are being collected using this simulant solution. We anticipate that we will obtain all the data needed by the middle of November and send a draft of the final report by the first week of December 1994.

Work performed:

	Hours
Principal Investigator	50 - 40
Support Scientist	360
Clerical	20

Data and Results from Distilled Water

with 4 Rotors

t_{av}	U_{av}	Flux	E_r	E_c	E_t
93	2570	2.47	37.0	27.7	64.7
96	2504	2.91	31.4	24.5	55.9
97	2067	2.87	32.1	25.4	57.5
100	2527	3.16	29.0	25.4	54.3
107	2209	3.63	25.1	24.5	49.6
107	2512	3.66	24.9	22.2	47.1
108	2304	3.83	24.1	22.6	46.7
109	2382	3.97	22.6	21.9	44.5
113	2354	4.09	22.8	23.7	46.5
113	2482	4.25	21.5	22.4	43.9
114	2488	4.37	20.9	23.0	43.9
116	2399	4.58	20.5	22.8	43.3
116	2394	4.55	21.1	22.9	44.0
121	2384	4.92	19.7	23.4	43.1
125	2558	5.63	17.4	23.5	40.9
125	2373	5.27	18.6	25.5	44.1
125	2491	5.38	17.8	23.8	41.6
125	2852	5.43	18.1	25.9	44.0
127	2414	5.69	17.2	25.2	42.4
129	2410	5.71	17.2	26.8	44.0
130	2504	6.00	16.7	24.5	43.2
132	2495	6.59	15.6	25.3	40.9
139	2519	7.17	14.7	27.5	42.2
139	2580	7.33	13.8	27.4	42.1

with 5 Rotors

100	2626	3.13	26.8	21.6	48.4
105	2768	3.43	23.9	20.4	44.3
110	2572	4.07	21.1	20.3	41.4
115	2704	4.37	20.1	20.2	40.3
124	2603	5.29	16.4	20.2	36.6
133	2668	6.23	15.5	23.8	39.3

t_{av}; Deg. F
U_{av}; Btu/hr F ft^2
Flux; lbs/hr ft^2
E_r; Whr/gal
E_c; Whr/gal
E_t; Whr/gal

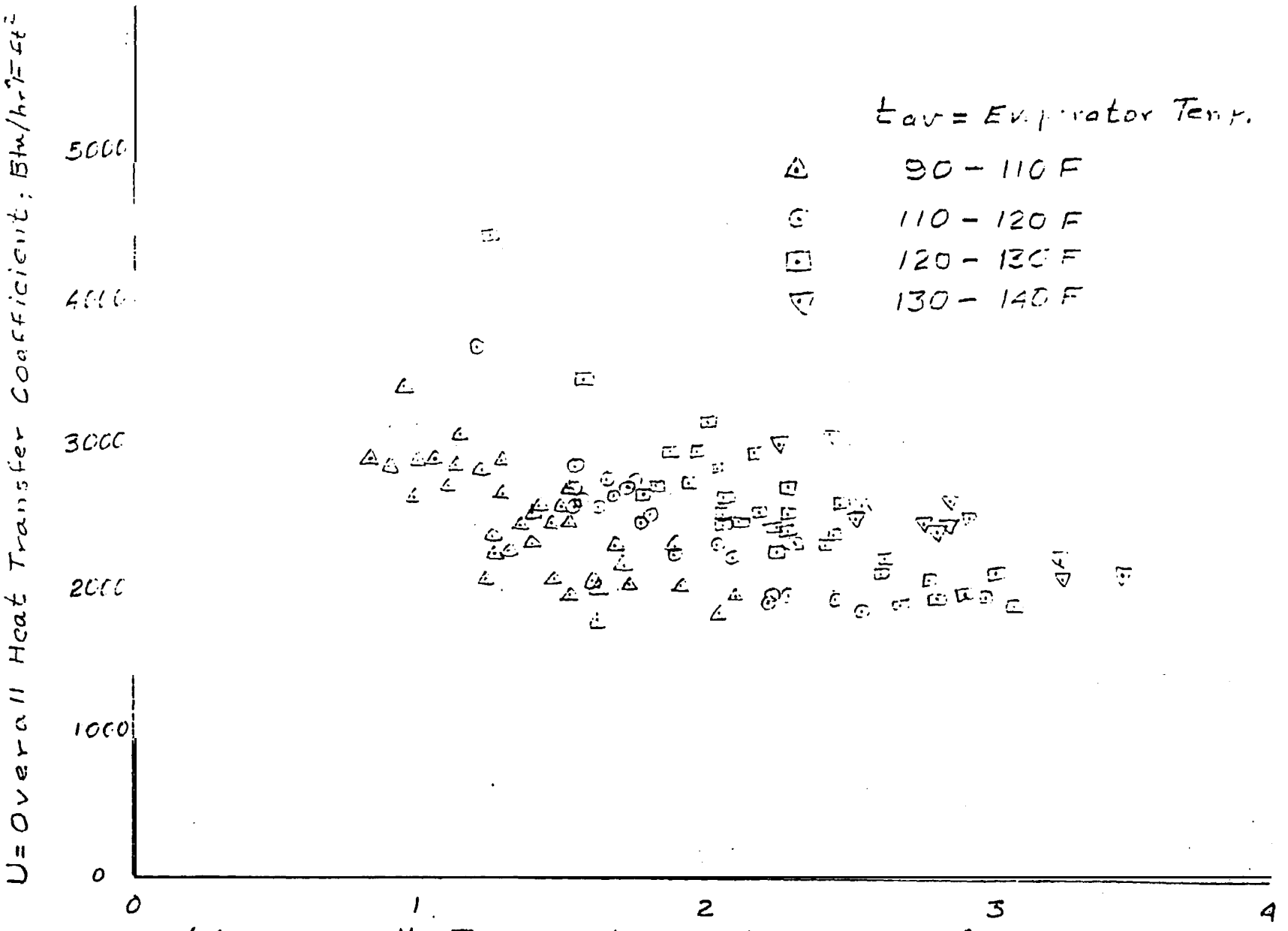

Fig. 1 Overall Heat Transfer Coefficient as Function of Lt for the Evaporator

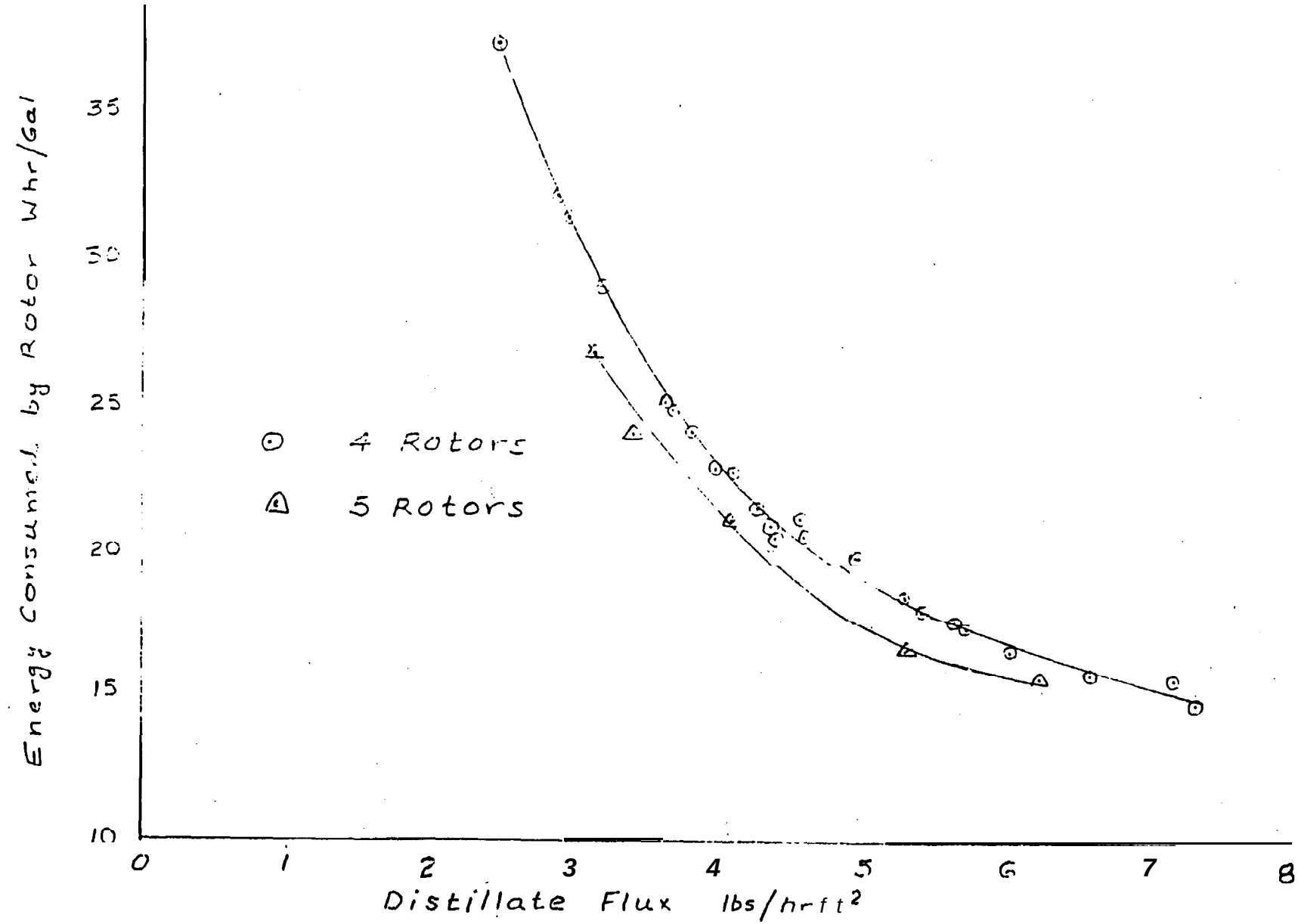

Fig. 2 Energy Consumption by Rotor as a Function of Flux

Appendix B

Data and Computed Results

Page 36 is a copy of a data sheet for runs made on November 14, 1994 for the simuiant solution and page 37 is a copy of a computer printout that shows data and results calculated for the data collected at 17:00 hour. In page 37, RoMo indicates rotor motor speed (1160 t-pm). The rotors are rotating at about 400 rpm through timing belts and pulleys. The two columns under temperature show the readings taken and the corresponding calculated temperatures for the indicated stations. Stations 1 through 5 show, respectively, the temperatures in the evaporator space in effects through 5 while stations 6 through 10 show, respectively, the temperatures in the condenser space in effects 1 through 5. Station 11 shows the temperature of the compressed vapor prior to entering the condenser space in effect 1. Station 12 measures the ambient air temperature close to the evaporator while T_{amb} indicates the ambient temperature in the building.

$T_c - T_e$ shows the measured temperature difference across the heat transfer surface in each of the effects. For example for effect 1, $T_c - T_e$ = 132.70 - 130.55 = 2.15" F.

The column under O.H.T.C. indicates the calculated values of U using Eq. 8 for each of the effects. The value 2601.7 is the average value of U for the five 'effects. The value of Dt,, = 2.10" F is the average value of $T_c - T_e$ for the five effects.

The values under temperature drop indicates the temperature drop from the evaporator in one effect to the condenser in the following effect. For example the temperature drop from effect 2 to the condenser in effect 3 is 128.70 - 128.29 = 0.41" F (difference between 0.41 and 0.42 shown on printout is due to truncation in the program). This difference is due to the effects of boiling point elevation, pressure drop, and errors in instrumentations.

TSAT(5) indicates the calculated saturation temperature corresponding to measured absolute pressure in effect 5.

The values under total mass balance indicates measurements and calculations. R_c, R_{fc}, and R_{fb} show rotameter readings. R_b shows the flow rate of the brine from the evaporator. This was calculated by measuring the time required (33.6 sec) to fill a calibrated 100 ml flask. The condensate rate was calculated by measuring the time in seconds (121.2 Sec) to collect 2.18 gal of condensate. The density of the brine was calculated by weighing the 100 ml brine collected in the 100 ml flask. The feed rate was calculated by adding the brine rate and condensate rate. The product flux (4.73 lbs/hrft^2) was calculated by dividing the distillate rate (539.2 lbs/hr) by the total heat

transfer area (113.95 ft").

The values under salt balance show feed salinity, brine salinity, brine density calculated from Eq. 7, condensate salinity, and brine salinity, S,, calculated from density and salinity correlations by Fabuss.

The boiling point elevation was calculated from salinity of the brine using the correlations by Fabuss. S,,(2) is the salinity in effects 1 and 2, $S_b(4)$ is the salinity in effects 3 and 4 and $S_b(5)$ is the salinity of the brine in effect 5. The boiling point elevation BPE(2) is due to salinity in effect 2, BPE(4) is due to salinity in effect 4 and **BPE(5)** is due to salinity in effect 5. The total boiling point elevation is the sum of the boiling point elevations in effects 1, 2, 3, 4, and 5 and is equal to **2BPE(2)** + **2BPE(4)** + BPE(5). The value T(5) • TSAT(5) should be equal to BPE(5) for an ideal system with noncondensible gases removed from effect 5.

The volumetric flow through the compressor was calculated by multiplying the condensate flow rate by the specific volume of the vapor in the fifth effect divided by the number of effects. The isentropic efficiency of the compressor was calculated as the ratio of the isentropic work per unit of product from the plant divided by the actual energy consumed by the compressor per unit of product from the plant. Compressor work ratio is calculated to show the ratio of heat gain by the vapor through compression to the actual work of compression.

Energy consumption by the rotor is calculated by dividing the measured power input to the rotor by the condensate rate. The number in parentheses shows the power meter reading. Energy consumption by the compressor is calculated in a similar manner, however, the value'in parenthesis show the total power input to the rotary phase convertor which includes power consumed by the rotary phase convertor (800 Watts) and compressor drive (2075 Watts). The last entry represents the total energy consumed by both rotors and compressor drive motors.

WRT

WATER REUSE TECHNOLOGY

Data Sheet For
100 gph Evaporator

Date: 11/4/94
Ref. No.: DOIBOR
Set No.: 25
Feed Type: Solution A
Feed TDS: 10000 ppm
Comp Speed: 3756 rpm

Time	14:00	14:30	[illegible]	16:30	17:00					
E1 (mV)	130.73	132.89	[illegible]	130.94	130.60					
E2 (mV)	129.54	136.66	128.82	128.96	128.74					
E3 (mV)	125.47	127.65	126.05	126.24	126.09					
E4 (mV)	[illegible]	125.26	123.77	123.91	123.96					
E5 (mV)	119.96	121.85	120.34	120.79	119.74					
E6 (mV)	[illegible]	134.72	132.87	132.91	132.71					
E7 (mV)	[illegible]	131.86	129.91	129.81	129.71					
E8 (mV)	127.52	127.60	127.81	127.72	127.70					
E9 (mV)	[illegible]	127.68	126.31	126.05	125.92					
E10 (mV)	[illegible]	134.37	[illegible]	133.96	133.81					
E11 (mV)	119.02	119.66	[illegible]	119.76	119.45					
E12 (mV)	79.56	[illegible]	[illegible]	79.69	79.45					
Amb. Temp. (F)	[illegible]	70	[illegible]	72	72					
DP Cell Reading	—	—	—	—	—					
DP Cell Zero	—	—	—	—	—					
DP (in. H2O)	.37	.35	.145	.23.7	.145					
Hg mano. (mm Hg)	76	77	74	74	75					
Rc (percent.)	37	41	36	38	38					
Rfc (per[illegible])	36	37	31	30	30					
Rfb (cc/min.)	0	750	700	800	800					
Rb[illegible] (cc/min.)	[illegible]	[illegible]	195	186	326 179					
Rotor Power (Watts)	1320	1330	1325	1290	1290					
Comp Power (Watts)	3710	3720	3660	3760	3675					
Cond Timer (sec.)	118.2	119.7	120.1	121.0	121.2					
Cond. TDS (ppm)	[illegible]	10	[illegible]	10	15					
Brine TDS (ppm)										
Brine Weight (g/cm³)	1.1051	1.1254	1.1176	1.1518	1.1584					
	A	B	A	A						

VENTS : 1/4" [illegible] 1/4" ALL

WATER REUSE TECHNOLOGY

Performance of RotoFilm 5100 advanced evaporator module
Data Redux Program: RF511194

Feed Name: Solution A
Comp Speed(rpm): 1750
Ave RoMo Speed(rpm): 1160
No of Effects: 5

Ref no: DOIBOR
Set Time: 1700
Date: 11/14/94
By: mt

STATION NO.	TEMP mV\F	EFFECT NO	Tc-Te (F)	O.H.T.C. BTU/hrft2F
1	130.60\130.55	1	2.15	2294.0
2	128.74\128.70	2	1.28	3767.5
3	126.09\126.49	3	1.80	2683.6
4	123.88\123.86	4	1.65	2930.9
5	119.74\119.33	5	3.64	1332.7
6	132.71\132.70			2601.7\ave.
7	129.71\129.98			
8	127.70\128.29			
9	125.92\125.51			
10	122.81\122.97			
11	187.45\189.56			
12	79.45\ 79.90			
Tamb	\ 72.0			

Otav

2.10

TEMP. DROP (F) EVAP. TO COND.		
1	2	0.57
2	3	0.42
3	4	0.97
4	5	0.89

TSAT(5) = 118.7764
P(mm Hg) = 84.46499

TOTAL MASS BALANCE
(Rc=38% \ Rfc=30% \ Rfb= 800ml/min \ Rb= 179ml/min \ Timer=121.2sec)
Distillate: 64.75 gal/hr = 539.2 lb/hr =1554.1 gpd (4.73 lbs/hr.ft2>
F e e d : 67.59 gal/hr = 566.6 lb/hr
Brine : 2.84 gal/hr = 27.4 lb/hr <Recovery = 95.2 percent>

SALT BALANCE
Feed Salinity = 10000 ppm
Brine Salinity = 2069'97 ppm [Sb(dens) = 179681 ppm]
Brine Density = 1.158 g/ml
Condensate Salinity = 75.0 ppm

Total Boiling Point Elevation = 4.16 F
Sb(2) = 16,147 ppm BPE(2) = 0.17 F
Sb(4) = 41,903 ppm BPE(4) = 0.54 F
Sb(5) = 206,997 ppm BPE(5) = 2.73 F
T(5) - TSAT(5) = 0.56 F

Volumetric Flow Through Compressor = 371.7 cu.ft./min.
Isentropic Compressor Efficiency = 44.4 percent
Compressor Work Ratio = 92.80 percent

$W_s = 14.23$

ENERGY CONSUMPTION
Rotor = 19.92 kWhr/kgal (1290 Watts)
Compressor = 32.05 kWhr/kgal (2875 Watts)
Total = 51.97 kWhr/kgal

REMARKS > same as prev.

Appendix C

Sample Calculations

Overall heat transfer coefficient U from Equation 8.

$U = \dot{m}r/A\,Dt = (539.2/5)(91042.7)/(22.79x2.15)$
$U = 2294\ Btu/^{\circ}Fhrft^2$

The saturation temperature t_s in this pressure range is correlated by:

$$t_s = -2.1955P_s^2 + 25.024P_s + 59.8401$$

Where P_s is absolute pressure in $in.H_g$ and t_s in $^{\circ}$ F.

$P_s = 85/25.4 = 3.3465\ in.H_g$
$t_s = 118.995^{\circ}$ F

Distillate rate = calibrated volume/time
calibrated volume = 2.18 gal
Distillate rate = 2.18x3600/121.2 = 64.75 gal/hr
Flux = distillate rate/total area = 539.2/(5x22.79)
Flux = 4.73 $lbs/hrft^2$
Brine rate = 27.4 lbs/hr
Feed rate = 27.4 + 539.2 = 566.6 lbs/hr

Brine salinity from Equation 7.
$S_b = m_f S_f / m_b$ = 566.6 x 10,000/27.4 = 206788 ppm
Brine density = brine weight/100 ml = 115.84/100 = 1.1584 gm/ml

Energy consumption by compressor is:
E_c = (2875-800)/64.75 = 32.05 Whr/gal
Energy consumption by rotors is:
E_r = 1290/64.75 = 19.92 Whr/gal = 19.92 kWhr/kgal
Total energy consumption by rotors and compressor drives is:
$E_t = E_c + E_r$ = 51.97 kWhr/kgal

Density and Boilina Point Elevation

The density, d, of salt solutions is given by:

$d = (1000 + \Sigma m_i M_i)/(V_o + \Sigma m_i V_i)$ Eq. A2.13 Fabuss

m_i = molality of dissolved component i
M_i = molecular weight of component i
V_o = volume of 1000 gm of water at temperature t
V_i = apparent molal volume of dissolved component i

V_i is given by Fabuss as:

$$V_i = A_{oi} + B_{oi} I^{.5} \quad \text{Eq. A2.8}$$
$$I = 0.5\Sigma\, n_i \beta_i \quad \text{Eq. A2.9}$$

n_i = ionic concentration of component i
β_i = valence of component i

at 25" C, the values of A_{oi} and B_{oi} are:

Salt	A_{oi}	B_{oi}
Na Cl	17.0168	1.2365
Na_2SO_4	12.701	7.4425

The ionic concentration of the simulant solution consists of 3380 ppm Na', 1460 ppm Cl-, and 5160 ppm SO_4^-

Na'	$3380/23.00 = 146.957 \times 10^{-3}$	Eq/kg water
Cl^-	$1460/35.455 = 41.179 \times 10^{-3}$	Eq/kg water
SO_4^-	$5160/96.06 = 53.716 \times 10^{-3}$	Eq/kg water

For the solution to be neutral, the total equivalent of anions and cations must be the same. In order to do that, we add 1.654 x 10^{-3} Na^+ which is equivalent to adding 1.654 x 23 x 10^{-3} = 38 ppm. The resulting ionic concentration for each component is:

Na'	148.611×10^{-3}	Eq/kg water
Cl^-	41.179×10^{-3}	Eq/kg water
Na_2SO_4	53.716×10^{-3}	Eq/kg water

The total solid content for neutral solution is:

3418 + 1460 + 5160 = 10,038 ppm

For a concentration factor n, the ionic composition of the concentrated solution is:

Na^+	$148.61\,1n/(1000-10.038n)$	Eq/kg
Cl^-	$41.179n/(1000-10.038n)$	Eq/kg
SO_4^{--}	$53.716n/(1000-10.038n)$	Eq/kg

For a final concentration of 200,000 ppm, the value of n is:

$$n = 200{,}000/10038 = 19.9243$$

The final ionic concentration for each component is:

Na^+	3.7012	Eq/kg water .
Cl^-	1.0256	Eq/kg water
SO_4^{--}	1.3378	Eq/kg water

The ionic strength of the solution is:

$$I = (3.7012x1 + 1.0256x1 + 1.3378x4)/2 = 5.039$$

and it consists of 1.0256 gm mole/kg of NaCl and 1.3378 gm mole/kg of Na_2 SO,.

The apparent molar volume is calculated as:

$$V\ NaCl = 17.0168 + 1.71325(5.039)^{0.5} = 20.8626$$
$$V\ Na_2SO_4 = 12.3265 + 6.6135(5.039)^{0.5} = 27.1723$$

The density of water at 25" C is 0.9969 gm/ml

$$V_o = 1000/0.9969 = 1003.11 \text{ ml/kg}$$
$$\Sigma m_i V_i = 1.0256 \times 20.8626 + 1.3378 \times 27.1723 = 57.7478 \text{ ml/kg}$$
$$\Sigma m_i M_i = 1.0256 \times 58.455 + 1.3378 \times 142.06 = 249.994 \text{ ml/kg}$$
$$d = (1000+249.994)/(1003.11+57.7478) = 1.1783 \text{ gm/ml}$$

The vapor pressure, P, of the brine in the fifth effect is given by:

$$P = P_o (1 - \Sigma k_i m_i) \qquad \text{Eq. A2.18 Fabuss}$$

The value of k_i is calculated using the correlation constants from Table A2.10 Fabuss at 50" C

$$k\ NaCl = 38.490x10^{-3};\ k\ Na_2SO_4 = 31.853x10^{-3}$$
$$\Sigma k_i m_i = 38.490x10^{-3}(1.0256) + 31.853x1.3378x10^{-3} = 82.088 \times 10^{-3}$$

The saturation pressure at 50° C is taken from steam tables. Its value at this temperature is: P_o = 0.12349 bars.

The vapor pressure of the brine in the fifth effect is given by:

P = 0.12349(l-0.082088) = 0.11335 bars

The equivalent vapor pressure

$P_2 = P_o^2/P$ Eq. A2.20 Fabuss
$P_2 = (0.12349)^2/0.11335$ = 0.13453 bars.

At this pressure, the saturation temperature is calculated by interpolation

t_s = 51.732" C

Therefore, the boiling point elevation of this concentrated solution is:

a = 51.732 - 50 = 1.732" C (3.118" F)